PB-249 505

CONTROL OF RECLAMATION (SINTER) PLANT EMISSIONS USING ELECTROSTATIC PRECIPITATORS

John Varga, Jr.

Battelle Columbus Laboratories
Columbus, Ohio

January 1976

DISTRIBUTED BY:

NTIS

National Technical Information Service
U. S. DEPARTMENT OF COMMERCE

051010

PB 249 505

EPA-600/2-76-002
January 1976

Environmental Protection Technology Series

Reproduced by
NATIONAL TECHNICAL
INFORMATION SERVICE
US Department of Commerce
Springfield, VA. 22151

RESEARCH REPORTING SERIES

Research reports of the Office of Research and Development, U.S. Environmental Protection Agency, have been grouped into five series. These five broad categories were established to facilitate further development and application of environmental technology. Elimination of traditional grouping was consciously planned to foster technology transfer and a maximum interface in related fields. The five series are:

1. Environmental Health Effects Research
2. Environmental Protection Technology
3. Ecological Research
4. Environmental Monitoring
5. Socioeconomic Environmental Studies

This report has been assigned to the ENVIRONMENTAL PROTECTION TECHNOLOGY series. This series describes research performed to develop and demonstrate instrumentation, equipment and methodology to repair or prevent environmental degradation from point and non-point sources of pollution. This work provides the new or improved technology required for the control and treatment of pollution sources to meet environmental quality standards.

EPA REVIEW NOTICE

This report has been reviewed by the U.S. Environmental Protection Agency, and approved for publication. Approval does not signify that the contents necessarily reflect the views and policies of the Agency, nor does mention of trade names or commercial products constitute endorsement or recommendation for use.

This document is available to the public through the National Technical Information Service, Springfield, Virginia 22161.

TECHNICAL REPORT DATA
(Please read Instructions on the reverse before completing)

1. REPORT NO. EPA-600/2-76-002	2.
3. RECIPIENT'S ACCESSION NO.	
4. TITLE AND SUBTITLE: Control of Reclamation (Sinter) Plant Emissions Using Electrostatic Precipitators	5. REPORT DATE: January 1976
	6. PERFORMING ORGANIZATION CODE
7. AUTHOR(S): John Varga, Jr.	8. PERFORMING ORGANIZATION REPORT NO.
9. PERFORMING ORGANIZATION NAME AND ADDRESS: Battelle-Columbus Laboratories, 505 King Avenue, Columbus, Ohio 43201	10. PROGRAM ELEMENT NO.: 1AB015; ROAP 21AQR-042
	11. CONTRACT/GRANT NO.: 68-02-1323, Task 32
12. SPONSORING AGENCY NAME AND ADDRESS: EPA, Office of Research and Development, Industrial Environmental Research Laboratory, Research Triangle Park, NC 27711	13. TYPE OF REPORT AND PERIOD COVERED: Final; 3/15-8/15/75
	14. SPONSORING AGENCY CODE
15. SUPPLEMENTARY NOTES	

16. ABSTRACT: The report briefly reviews the sintering process as it applies to the U.S. integrated iron and steel industry. The review includes data on characteristics of the emissions, and a list of all the iron and steel reclamation (sinter) plants in the U.S., their annual capacity, and the types of emission control equipment used. The report contains a detailed discussion of the theoretical and practical aspects of designing both wet and dry electrostatic precipitators (ESPs) to control the sinter machine windbox emissions. It gives design specifications for a proposed wet ESP installation on a large modern sinter plant.

KEY WORDS AND DOCUMENT ANALYSIS

17. a. DESCRIPTORS	b. IDENTIFIERS/OPEN ENDED TERMS	c. COSATI Field/Group
Air Pollution Iron and Steel Industry Electrostatic Precipitators Reclamation Sintering Sintering Furnaces Design Specifications	Air Pollution Control Stationary Sources Sinter Plants Sinter Machine Windbox	13B 13H 13A 11F

18. DISTRIBUTION STATEMENT: Unlimited	19. SECURITY CLASS *(This Report)*: Unclassified	21. NO. OF PAGES: 81
	20. SECURITY CLASS *(This page)*: Unclassified	22. PRICE: 5.00

EPA Form 2220-1 (9-73)

CONTROL OF
RECLAMATION (SINTER) PLANT EMISSIONS
USING ELECTROSTATIC PRECIPITATORS

by

John Varga, Jr.

Battelle-Columbus Laboratories
505 King Avenue
Columbus, Ohio 43201

Contract No. 68-02-1323, Task 32
ROAP No. 21AQR-042
Program Element No. 1AB015

EPA Task Officer: Robert C. McCrillis

Industrial Environmental Research Laboratory
Office of Energy, Minerals, and Industry
Research Triangle Park, NC 27711

Prepared for

U.S. ENVIRONMENTAL PROTECTION AGENCY
Office of Research and Development
Washington, DC 20460

January 1976

ia

SUMMARY

The general aspects concerning the production of sinter in the integrated iron and steel industry are discussed as an introduction to the discussion on the control of emissions from sinter-plant windboxes. Some technical design information is presented, as are data pertaining to the characteristics of emissions. A limited amount of information is provided concerning the procedures used to develop the required design criteria for the construction of electrostatic precipitators.

"This report was prepared in response to Item AM-1-3 of the Protocol of the First Working Meeting of the USA/USSR Task Force on Abatement of Air Pollution from the Iron and Steel Industry."

РЕФЕРАТ

Рассматриваются проблемы общего характера, возникающие при производстве агломерата в металлургической промышленности. Эта работа является введением в рассмотрение проблемы контроля выбросов из воздуходувок агломерационных фабрик. Дан материал технически-конструктивного характера, а также данные относящиеся к характеристикам выбросов. Представлены некоторые данные о методике разработки конструктивных критериев, необходимых для создания электрофильтров.

Этот доклад подготовлен в согласии с пунктом АМ-I-3 Протокола Первого Рабочего Совещания Рабочей Группы США/СССР по Борьбе с Загрязнением Воздушного Бассейна Металлургической Промышленностью.

TABLE OF CONTENTS

	Page
I. INTRODUCTION	1
II. TRENDS OF SINTER USE IN THE U. S. INTEGRATED IRON AND STEEL INDUSTRY	3
III. AIR POLLUTION CONTROL FOR RECLAMATION (SINTER) PLANTS	5
IV. CHARACTERIZATION OF EMISSIONS	11
V. RECLAMATION (SINTER) PLANT ELECTROSTATIC PRECIPITATOR DESIGN CHARACTERISTICS	21
Basic Electrostatic Precipitator Parts	21
Dry-Dust-Collection Fundamentals	23
Factors Affecting Dry Electrostatic Precipitator Operation	28
Dry Electrostatic Precipitator Design Methods	40
Wet Electrostatic Precipitator	50
Wet-Dust-Collection Fundamentals	50
Horizontal-Flow Wet Electrostatic Precipitator	58
Range of Applications	60
Reclamation (Sinter) Plant Design Specifications	61
Reclamation (Sinter) Plant Electrostatic Precipitator Design Data	61
VI. REFERENCES	71

LIST OF FIGURES

Figure 1. Trend in the use of sinter in the metallic burden of U. S. blast furnaces	4
Figure 2. Trend in the use of limestone in blast furnace sinter as shown by the use of limestone in the sinter mix	4

LIST OF FIGURES
(Continued)

		Page
Figure 3.	Effect of temperature and sinter basicity on resistivity of sinter-plant particulate	8
Figure 4.	Effect of sinter basicity on the collection efficiency of an electrostatic precipitator	9
Figure 5.	Flow diagram of a typical reclamation (sinter) plant	12
Figure 6.	Size distribution of particulates entering dust collecting systems	14
Figure 7.	Size distribution of sinter plant particulates collected by different types of dust collecting equipment	14
Figure 8.	Size distribution of particulates released to the atmosphere after passing through sinter plant cleaning systems	16
Figure 9.	Particle-size distribution of sinter machine dust	17
Figure 10.	Two possible rectifier circuits for an electrostatic precipitator	22
Figure 11.	Typical duct electrostatic precipitator	23
Figure 12.	Voltage waveform for unfiltered half-wave and full-wave rectification	29
Figure 13.	Waveform in electrostatic precipitator after discharge	30
Figure 14.	Dust-collection efficiency as related to peak voltage for a typical electrostatic precipitator	33
Figure 15.	Electrostatic precipitator efficiency as affected by gas flow	34

LIST OF FIGURES
(Continued)

Page

Figure 16. A typical relationship between dust resistivity and temperature for a gas improperly conditioned for the 93 to 204 C (200 to 400 F) range 39

Figure 17. Relationship between precipitation-rate parameter ω and resistivity of fly ash 42

Figure 18. Relationship between the sulfur content in electric utility plant fuel and the precipitation-rate parameter ω at 149 C (300 F) 44

Figure 19. Collection efficiency as affected by power rate per unit gas flow 45

Figure 20. Relationship between collection efficiency and sectionalization (number of bus sections per unit gas flow) for utility fly-ash precipitators . . 45

Figure 21. Relationship between precipitation-rate parameter ω and power density for fly ash precipitators 48

Figure 22. Electrical resistivity of reclamation (sinter) plant dust as affected by gas temperature and sinter mixture 67

Figure 23. Relationship between the sulfur content in electric-utility-plant fuel and the precipitation-rate parameter 67

Figure 24. Collection efficiency as affected by the ratio of collection area to gas velocity 69

LIST OF TABLES

Table 1. Reclamation (Sinter) Plants in the U. S. Integrated Iron and Steel Industry 6

Table 2. Sinter-Mix Composition 13

LIST OF TABLES
(Continued)

		Page
Table 3.	Composition of Particulate Emissions	15
Table 4.	Gaseous Emissions From Reclamation (Sinter) Plants	16
Table 5.	Size Distribution of Particulates Entering the Atmosphere From an Electrostatic-Precipitator-Controlled Sinter Plant	18
Table 6.	(Plant D) Gaseous Emissions Entering the Atmosphere From an Electrostatic Precipitator Controlled Sinter Plant	19
Table 7.	Representative Precipitation Rates, ω, for Various Applications	42
Table 8.	Number of Rappers in Electrostatic Precipitators for Various Applications	46
Table 9.	Nomenclature for Wet-Dust-Collection Fundamentals	53
Table 10.	Equipment Specifications	62
Table 11.	Reclamation (Sinter) Plant Data for Figure 22 . .	68
Table 12.	Reclamation (Sinter) Plant Electrostatic-Precipitator Characteristics	70

I. INTRODUCTION

The use of sintering processes to improve the characteristics of blast-furnace burden materials has long been an accepted practice in the integrated iron and steel industry. In recent years, as the need increased for recovering the metallic values from the dusts and scrap generated by the various iron and steelmaking processes, the plants have become known as reclamation plants, rather than as sinter plants.

A major problem in the control of emissions from a reclamation plant is the minimizing of emissions from the windbox of the sintering machines. The integrated iron and steel industry in the United States has used many types of control equipment in attempts to control emissions from sinter machines, with electrostatic precipitators, cyclones, and scrubbers being used on 93 percent of the sinter machines.

This Protocol Report discusses the application of electrostatic precipitators for the control of sintering-machine windbox emissions, and is based on available published information and additional information supplied by iron and steel companies.

II. TRENDS OF SINTER USE IN THE U. S. INTEGRATED IRON AND STEEL INDUSTRY

The integrated iron and steel industry of the United States operates 45 reclamation plants having a total of 72 sintering strands. The reclamation plants consist of 29 single-strand plants, 10 double-strand plants, 3 plants having 3 strands, 2 plants with 4 strands, and 1 plant with 6 strands. During 1974, the integrated iron and steel industry produced 36,985,182 metric tons (40,769,185 net tons) of blast furnace sinter.(1) The greatest tonnage of sinter was produced in 1964 and amounted to 49,518,907 metric tons (54,585,251 net tons). The trend in the percentage of sinter used in the metallic burden (iron ore + pellets + sinter) of blast furnaces is shown in Figure 1. The year 1961 was the year of greatest percentage use of sinter, 44 percent of the blast-furnace metallic burden. The decrease in use of sinter has been caused by the increase in production and use of pellets in the U. S. integrated iron and steel industry.

Although there has been a decline in the use of sinter in blast furnaces, the sinter that is being made is more and more of the self-fluxing variety (high basicity). The trend in increased basicity is illustrated by the increased use of limestone in the sinter mix as shown in Figure 2. Integrated iron and steel plants that are heavily committed to the use of self-fluxing sinter are using limestone in amounts even greater than the average illustrated in Figure 2.

Preceding page blank

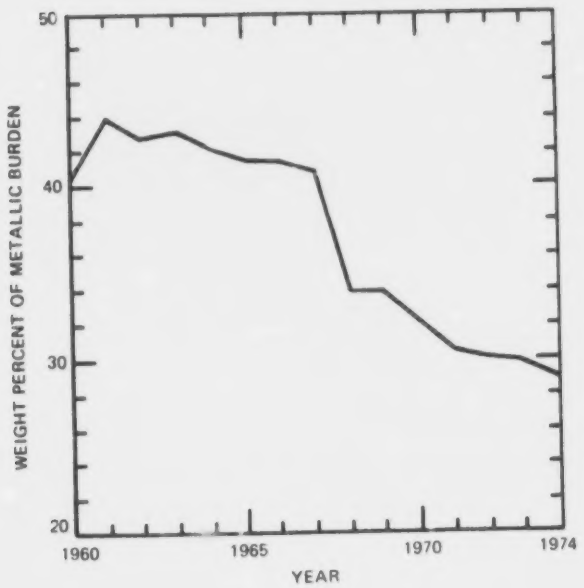

Figure 1. Trend in the use of sinter in the metallic burden of U.S. blast furnaces

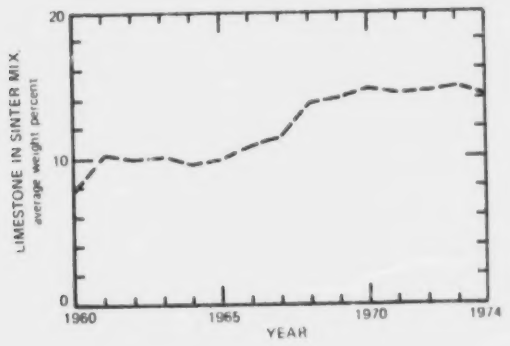

Figure 2. Trend in the use of limestone in blast furnace sinter as shown by the use of limestone in the sinter mix

III. AIR POLLUTION CONTROL FOR RECLAMATION (SINTER) PLANTS

The emissions associated with reclamation-plant operation are primarily particulates that become entrained in the combustion air as it is drawn through the sinter mix into the windbox. However, sulfur dioxide, carbon monoxide, and hydrocarbons may also occur in the emissions, depending on the operating practice of a particular reclamation plant. Sulfur dioxide may originate from sulfur contained in the ore and the coke that are used as part of the sinter mix and in the fuel used to ignite the mixture, and it may also originate from the sulfur contained in machining oils that adhere to steel turnings, which are recycled to a reclamation plant to recover the metallic values. Machining oils are also the principal source of hydrocarbons in reclamation-plant windbox emissions.

Electrostatic precipitators, scrubbers, and cyclones are the principal means for controlling emissions from the windboxes of sinter machines, while baghouses are the preferred method for control at other reclamation-plant locations, such as sinter discharge, crushing, screening, and material-transfer points. The reclamation plants in the U. S. integrated iron and steel industry are listed in Table 1. The distribution of air pollution control equipment used on the windbox of sinter machines is as follows:

Type of Control	Number
Electrostatic Precipitator	22
Cyclones	11
Scrubbers	9
Baghouse	1
Steam Ejector	1
Mechanical	1
Total	45

TABLE 1. RECLAMATION (SINTER) PLANTS IN THE U. S. INTEGRATED IRON AND STEEL INDUSTRY

Company	Location	No. of Strands	Estimated Annual Capacity, net tons	Ignition Fuel	Air Pollution Control			References
					Machine Windbox	Machine Discharge	Crushing & Screening	
Alan Wood Steel Co.	Swedeland, Pa.	3	475,000	Coke-oven gas	Scrubber	Baghouse		(2, 3)
Bethlehem Steel Corp.	Bethlehem, Pa.	4	2,400,000	Natural gas	ESP	Baghouse	Baghouse	(4, 5, 6, 7)
	Johnstown, Pa	2	1,100,000	Natural gas	ESP	Scrubber	Scrubber	(8, 9)
J & L Steel Corp.	Aliquippa, Pa.	1	2,700,000	Coke-oven gas	Cyclones			(10, 11, 12)
U. S. Steel Corp.	Braddock, Pa.	1	600,000	Mixed gas	ESP			(13)
	McKeesport, Pa.	1	325,000	Natural gas	Scrubber			(14)
	Rankin, Pa.	1	600,000	Natural gas	ESP			(15)
	Saxonburg, Pa.	1	1,500,000	Natural gas	ESP			
		1	1,500,000	Natural gas	ESP		Baghouse	(16, 17)
		1	1,500,000	Natural gas	ESP			
	Fairless Hills, Pa.	2	3,000,000	Mixed gas	ESP			(13)
W-P Steel Corp.	Monessen, Pa.	1	500,000	Coke-oven gas	ESP			(18)
Bethlehem Steel Corp.	Lackawanna, N. Y.	2	1,100,000	Coke-oven gas	ESP		Scrubber	(19)
J & L Steel Corp.	Star Lake, N. Y.	2	1,400,000	Fuel oil	Cyclones			(13, 20)
Bethlehem Steel Corp.	Sparrows Point, Md.	6	3,600,000	Coke-oven gas	ESP		Scrubber	(13, 21)
		1	4,250,000		Scrubber	Baghouse	Baghouse	(13, 22)
National Steel Corp.	Weirton, W. Va.	2	2,800,000	Coke-oven gas	Cyclones	Wet separators	Wet separators	(13, 23)
W-P Steel Corp.	E. Steubenville, W. Va.	1	550,000	Coke-oven gas	Scrubber			(24)
Armco Steel Corp.	Middletown, Ohio	1	900,000		Scrubber	Recycle	Baghouse	(25)
J & L Steel Corp.	Cleveland, Ohio	1	900,000	Natural gas	ESP	Multicyclones	Multicyclones	(13, 26)
Republic Steel Corp.	Cleveland, Ohio	1	400,000	Coke-oven gas	Cyclones			(13, 27, 28)
	Youngstown, Ohio	1	500,000	Coke-oven gas	Cyclones			(13, 28)
	Warren, Ohio	1	400,000	Coke-oven gas	Cyclones			(13, 28)
U. S. Steel Corp.	Lorain, Ohio	1	500,000	Natural gas	Cyclones			(13, 29)
	Youngstown, Ohio	1	1,500,000	Natural gas	ESP			(30)
Youngstown S & T Co.	Campbell, Ohio	2	800,000	Natural gas	Cyclones			(13, 31)
Armco Steel Corp.	Ashland, Ky.	1	800,000	Natural gas	Mechanical			(32)
National Steel Corp.	Ecourse, Michigan	1	2,000,000	Coke-oven gas	Scrubber			(33)
Inland Steel Co.	East Chicago, Ind.	1	1,200,000	Coke-oven gas	ESP			(34, 35)
U. S. Steel Corp.	Gary, Ind.	2	1,500,000	Mixed gas	ESP	Baghouse		(13)
		3	5,200,000	Natural gas	ESP	Baghouse	Baghouse	(36)
Youngstown S & T Co.	Indiana Harbor, Ind.	1	1,200,000	Natural gas	ESP			(13)
Bethlehem Steel Corp.	Burns Harbor, Ind.	1	2,000,000		Scrubber	Baghouse	Baghouse	(37)
Interlake Steel Corp.	South Chicago, Ill.	1	750,000	Coke-oven gas	ESP		Baghouse	(38, 39)
National Steel Corp.	Granite City, Ill.	1	1,000,000	Coke-oven gas	Scrubber	Cyclones	Baghouse	(40, 41, 42)
Republic Steel Corp.	South Chicago, Ill.	1	400,000	Coke-oven gas	Cyclones			(13)
U. S. Steel Corp.	South Chicago, Ill.	3	2,200,000	Natural gas	ESP		Baghouse	(43, 44)
I-H, Wisconsin Steel	South Chicago, Ill.	1	500,000	Coke-oven gas	Scrubber			(45)
Republic Steel Corp.	Gadsden, Ala.	1	500,000	Coke-oven gas	Cyclones			(13)
U. S. Steel Corp.	Fairfield, Ala.	4	2,500,000	Natural gas	ESP	Baghouse		(13)
Lone Star Steel Co.	Lone Star, Texas	1	300,000	Natural gas	Scrubber			(15)
Armco Steel Corp.	Houston, Texas	1	500,000	Coke-oven gas	Steam Ejector			(15)
CF & I Corp.	Pueblo, Colorado	2	900,000	Coke-oven gas	ESP	Baghouse		(13, 46, 47)
U. S. Steel Corp.	Geneva, Utah	2	800,000	Mixed gas	ESP	Scrubber		(13, 15)
Kaiser Steel Corp.	Fontana, Cal.	2	1,300,000	Coke-oven gas	Baghouse			(48, 49)

Most sintering operations that use electrostatic precipitators as control equipment for windbox emissions also use cyclones, or mechanical collectors, between the windbox and the fan. In the preceding tabulation, 10 sinter machines are listed as having cyclones for the control of windbox emissions. The cyclones are the only air pollution control devices on these 10 machines.

With respect to the control of emissions, developments in blast-furnace technology have created problems for the reclamation-plant operator. The increased use of high-basicity sinter introduces higher limestone additions to the sinter mixture. The relationship between temperature and resistivity for six different sinter-plant dusts is shown in Figure 3.[50] The effect of sinter basicity on the efficiency of an electrostatic precipitator is shown in Figure 4.[50] The variations in resistivity and the effects of basicity are the reasons that the control of sinter plant emissions is difficult. The problem of different resistivities may result in the installation of additional electrostatic-precipitator chambers, with one group designed to collect the iron oxide particulates and another group to collect the limestone particulates. In some instances, electrostatic precipitators were replaced by scrubbers to overcome the problem of different properties of the two types of emissions.

Integrated iron and steel plants that have facilities for making finished steel products, such as threaded pipe, generate oily machine turnings which are sent to the reclamation plant for recovery of the metallic values. The oil on the turnings creates problems in electrostatic precipitators, and in some cases hydrocarbons will pass through a scrubber system. Electrostatic-precipitator collector plates become coated with films of oil, which makes removal of the dusts difficult and in some cases impossible. If a steel plant is committed to the recovery of oily turnings in its reclamation plant, the trend is to use high-energy wet scrubbers for air pollution control, rather than electrostatic precipitators. The three newest reclamation plants under construction or recently placed into operation in the United States (those located at Bethlehem Steel Corporation's Sparrows Point and Burns Harbor plants, and the Armco Steel Corporation's plant at Middletown, Ohio) all have high-energy scrubbers as the primary air pollution control equipment on the sinter-plant windbox.[13, 22, 25, 37]

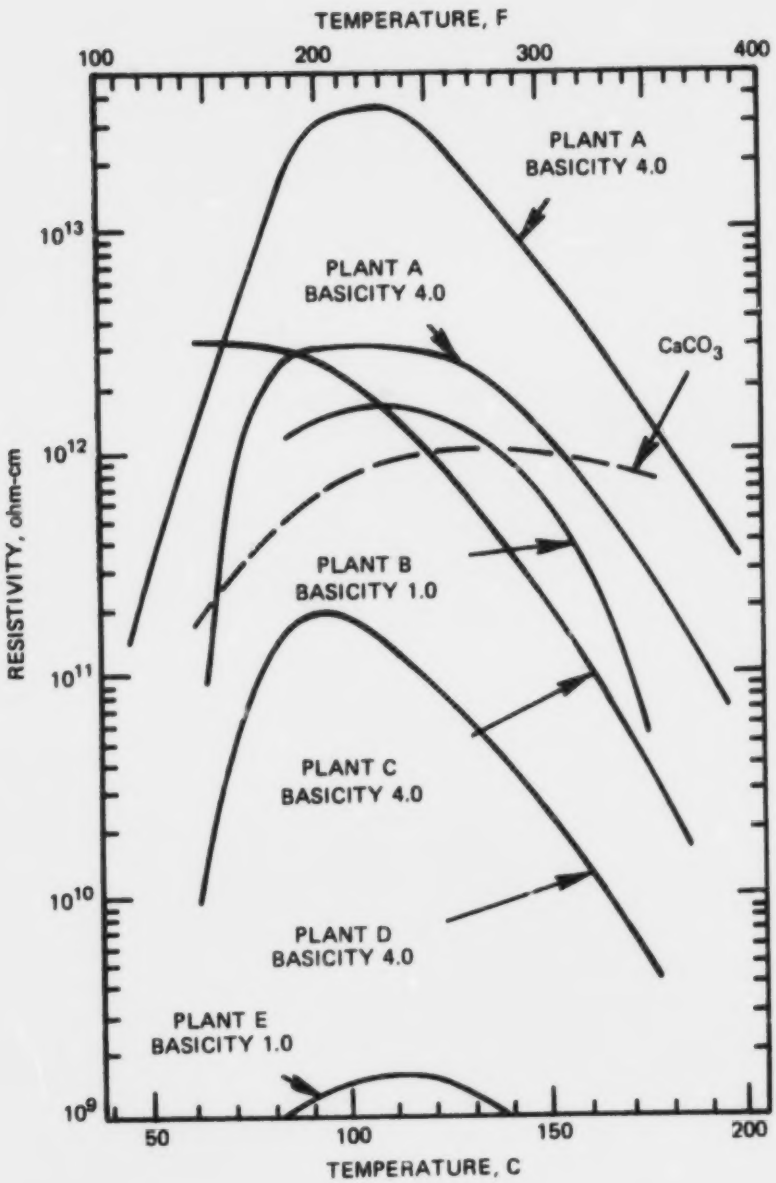

Figure 3. Effect of temperature and sinter basicity on resistivity of sinter-plant particulate

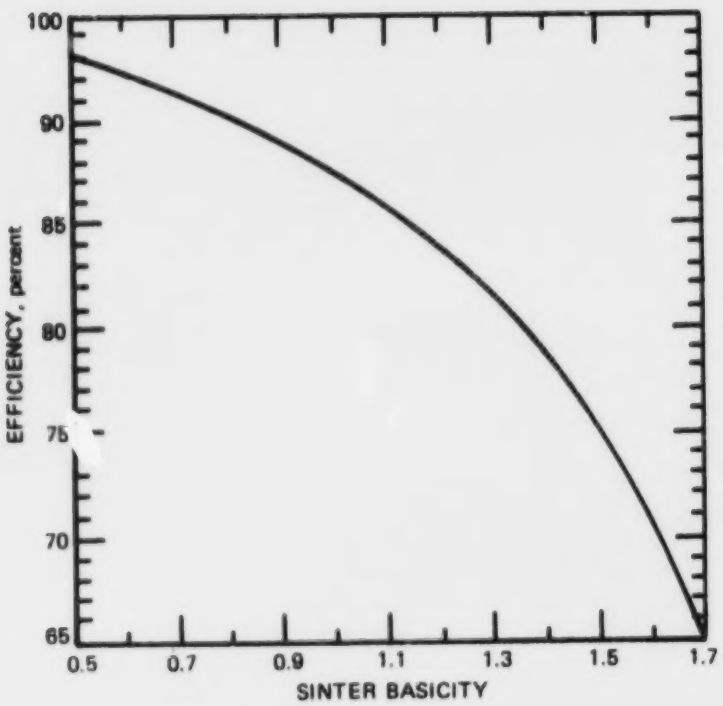

Figure 4. Effect of sinter basicity on the collection efficiency of an electrostatic precipitator

IV. CHARACTERIZATION OF EMISSIONS

Emissions from reclamation plants usually consist of the following: (1) minor amounts of dust generated in the handling and grinding of raw materials, (2) particul..es that are drawn down through the grate bars of the sintering machine, (3) combustion gases from ignition and firing of the sinter mix, and (4) dust generated during the cooling, crushing and screening operations. Points of emission are indicated in the flow sheet in Figure 5 for a typical reclamation plant. Circled numbers on the flow sheet are indexes to the circled numbers in the following discussion on the characterization of emissions.

(1) Iron Ore Dust. Particles are rounded to elongated in shape and can have a size as small as 2 microns. Larger particles are opaque, and red-orange when viewed under top light. Individual small grains are transparent and blood-red.[51] The particulates consist mostly of Fe_2O_3 or Fe_3O_4, some silica, and limestone, with a Mohs hardness of 5 and a specific gravity of 5.2.

(2) Limestone Dust. Primarily the mineral calcite. It is colorless, with light-transmitting characteristics varying from transparent to translucent. Because of their good cleavage, particles generally occur as rhombohedra. Fragments may also occur as prisms.[51] The Mohs hardness is 3 and the specific gravity 2.7.

(3) Coke Dust. Particles are opaque, irregularly shaped, quite porous, and rough with some straight, sharp edges. They are gray to black in reflected light and are about 90 percent carbon.[51]

(4) Combustion Products. Gases leaving the sintering strand are the result of the combustion of coke or coal in the sinter mix and of the fuels used to ignite the sinter mixture. Fuel for ignition is primarily coke-oven gas or natural gas, with some use of mixed gas or fuel oil. Hydrogen sulfide in the coke-oven gas and sulfur in the coke or coal in

Preceding page blank

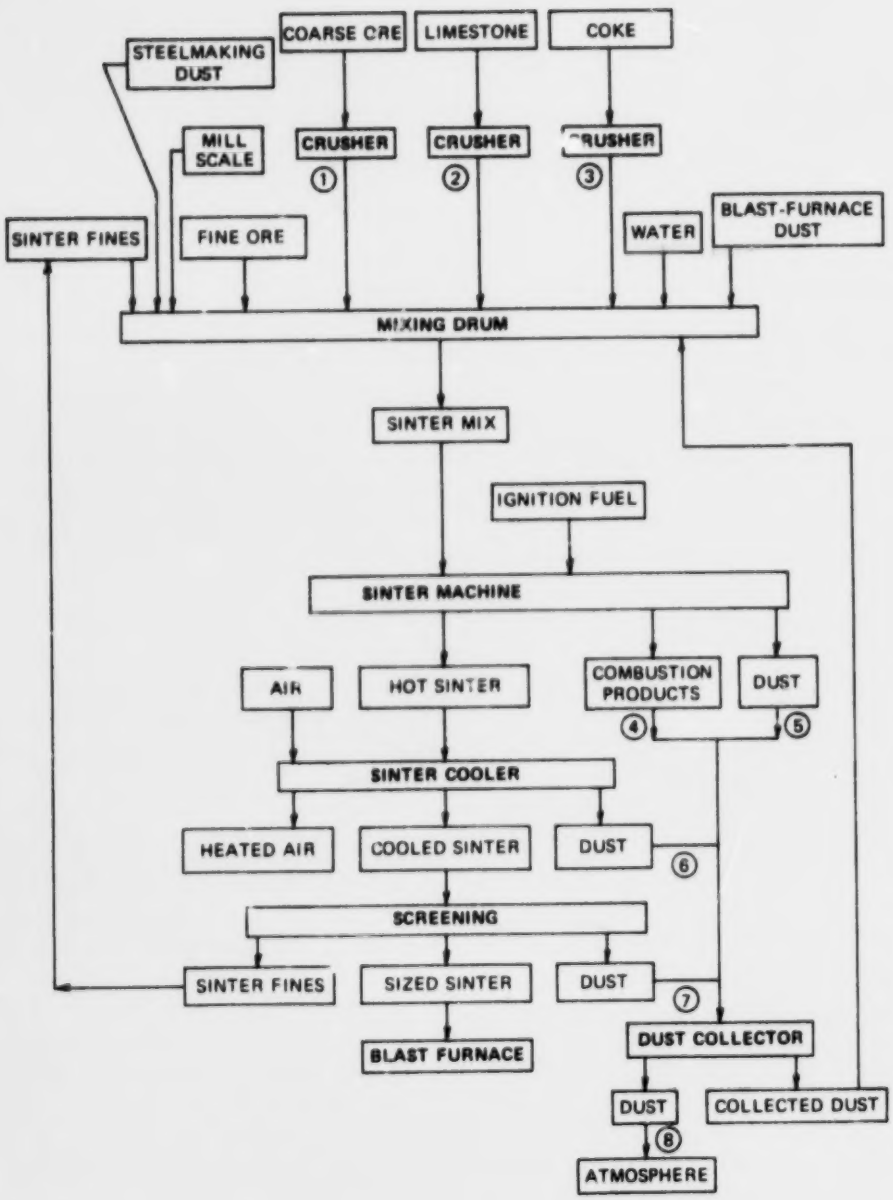

Figure 5. Flow diagram of a typical reclamation (sinter) plant.

the sinter mix can lead to sulfur dioxide emissions in the off-gas. Even though an excess of air is drawn through the sinter mix to assure oxidizing conditions, in most cases it is insufficient to burn the hydrocarbons completely in the sinter mix (hydrocarbons originating from oily turnings and volatiles in coal and coke); thus unburned hydrocarbons may be present in the sinter-plant off-gas. Incomplete combustion also produces carbon monoxide in the off-gas.

⑤ ⑥ ⑦ Sinter Dust. Dust may contain particles of iron oxides, calcite, iron-calcium silicates, and quartz. Iron oxide can be opaque, black, rounded particles of magnetite (Fe_3O_4) with angular faces and/or dense, rounded, elongated, and nearly spherical agglomerates of hematite (Fe_2O_3). Calcite occurs as smooth, rounded particles, and quartz as a transparent, rounded particle. The iron-calcium silicates are transparent, vitreous, colorless to yellow to green, and irregularly rounded with smooth surfaces.[51]

⑧ Atmospheric Emissions. Characterization of emissions to the atmosphere are discussed below, on the basis of work reported by plants in the U.S. integrated iron and steel industry.

Data pertaining to the sinter-mix composition from three sinter plants, the chemical compositions of particulate emissions, and the compositions of gaseous emissions are given in Tables 2, 3, and 4, respectively.[52, 53]

TABLE 2. SINTER-MIX COMPOSITION

weight percent

Sinter-Mix Components	Plant F	Plant G	Plant H
Iron ore	29.1		49.5
Dry blast-furnace dust	1.3	82.0	5.6
Blast-furnace filter cake	15.8		4.9
Melt-shop slag	6.5		0.0
Rolling-mill scale	11.5	0.0	7.6
Basic-oxygen-furnace dust	3.5	0.0	0.0
Miscellaneous dust	0.0	0.0	6.7
Limestone or dolomite	28.2	15.0	20.8
Coke	4.1	3.0	4.9

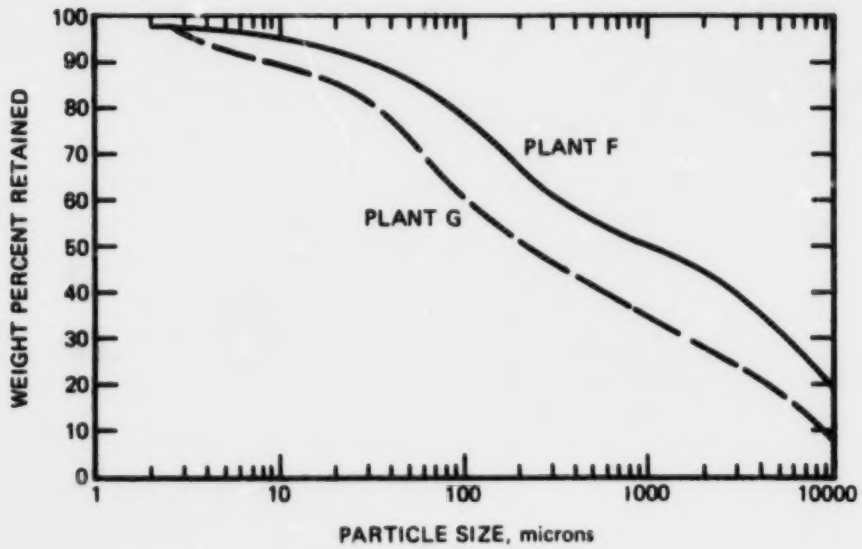

Figure 6. Size distribution of particulates entering dust collecting systems

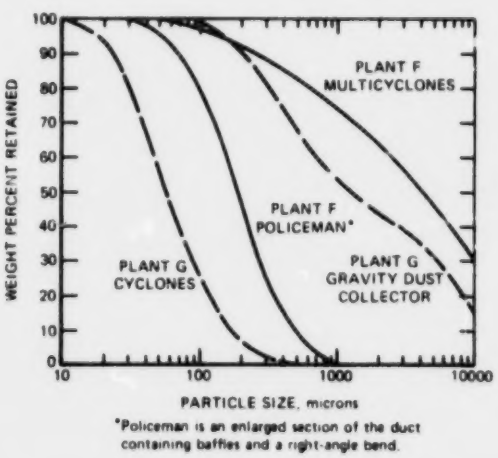

Figure 7. Size distribution of sinter plant particulates collected by different types of dust collecting equipment

TABLE 3. COMPOSITION OF PARTICULATE EMISSIONS

weight percent

Particulate Component	Plant F	Plant G	Plant H
Fe_2O_3	33.9	11.7	28.0
CaO	7.1	10.9	15.0
MgO	5.3	0.4	2.0
K_2O	5.2	0.6	8.1
SiO_2	4.8	2.4	4.6
Al_2O_3	2.6	4.3	2.5
Na_2O	1.6	0.8	0.0
ZnO	0.4	0.1	0.0
MnO	0.2	0.1	0.0
Chlorides	8.5	3.0	8.8
Sulfates	7.5	16.5	2.1
Hydrocarbons	7.4	36.9	0.0
Other	1.6	0.0	0.0
Loss on Ignition	13.9	12.3	28.9
Total	100.0	100.0	100.0

The size distributions of particulates entering the dust-collecting systems in Plants F and G are shown in Figure 6.[52] The size distributions of particulates collected by different dust-collection equipment in Plants F and G are shown in Figure 7[52], and the size distribution of particulates released to the atmosphere from Plants F, G, H and I are shown in Figure 8.[52, 53, 54]

Particle-size distributions of particulates entering a mechanical collector vary over a considerable range, as shown in Figure 9.[55] The size range of the particulates leaving the mechanical collector and entering the electrostatic precipitator is of a smaller magnitude than that of particulates entering the mechanical collector.

TABLE 4. GASEOUS EMISSIONS FROM RECLAMATION (SINTER) PLANTS

Gaseous Component	Milligrams per Cubic Meter			Volume Percent
	Plant F	Plant G	Plant H	Plant H
Sulfur dioxide	78.0	65.0	36-65	
Chlorides	80.0	32.0	5-44	
Fluorides	8.0	0.5	0.00	
Ammonia	0.0	2.6	0.00	
Carbon dioxide				3.4- 5.0
Carbon monoxide or illuminants				0.4- 0.9
Oxygen				16.5-18.1

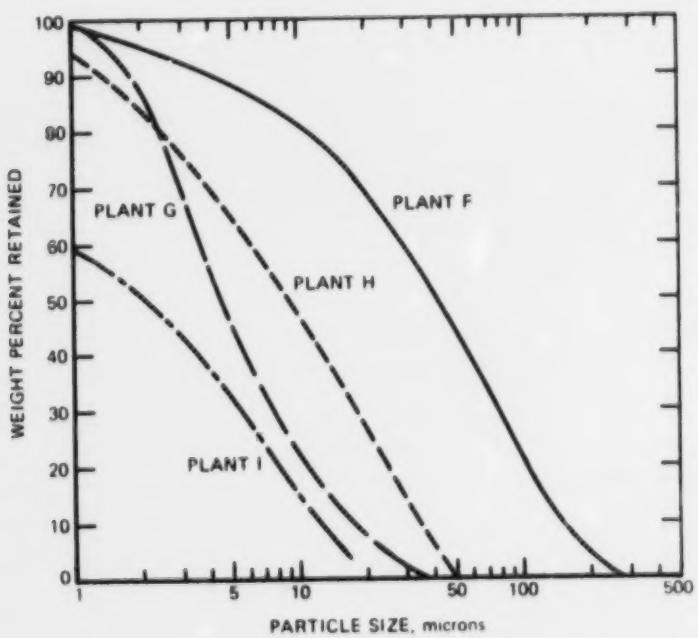

Figure 8. Size distribution of particulates released to the atmosphere after passing through sinter plant cleaning systems

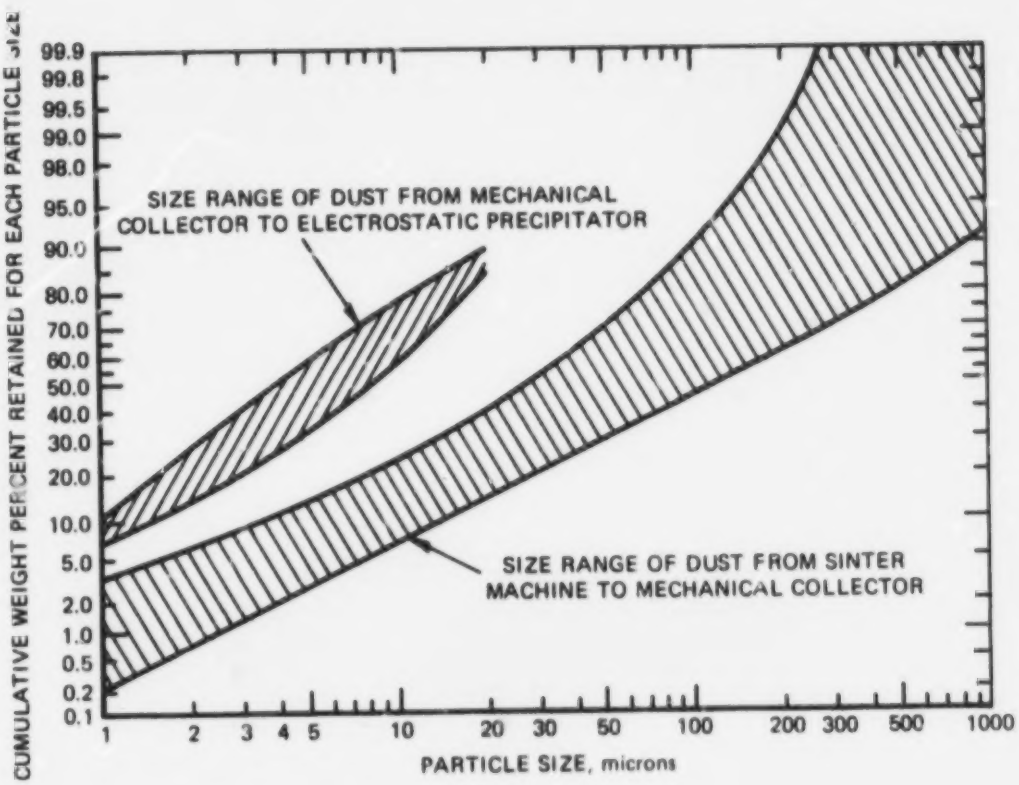

Figure 9. Particle-size distribution of sinter machine dust

During 1975, emission tests were made on a sinter plant having electrostatic precipitators as the windbox air pollution control system.[54] The sinter machine has four strands with an estimated production capacity of about 227 metric tons (250 net tons) per hour. The sinter-mix composition was as follows:

Sinter-Mix Components	Weight Percent
Iron ore	52
Reclaimed oily mill scale and flue dust	8
Reclaimed basic oxygen furnace slag	17
Limestone and dolomite	16
Coal	7
Total	100

The sinter produced has a basicity varying between 1.0 and 1.5, which is in the range of self-fluxing and superfluxing sinter, for the particular plant operation. Windbox exhausts are controlled by multiclones, followed by electrostatic precipitators. One electrostatic precipitator is used to control emissions from two sinter strands, and each is designed to operate at a gas flow rate of 10,903 m^3/min (385,000 acfm) at 118 C (245 F). The size distributions of particulates collected during two tests are given in Table 5.[54] The variation in the size distributions is not explained in the test report. However, this may have been caused by the day-to-day variations in the fineness of the materials charged to the sinter mix.

TABLE 5. SIZE DISTRIBUTION OF PARTICULATES ENTERING THE ATMOSPHERE FROM AN ELECTROSTATIC-PRECIPITATOR-CONTROLLED SINTER PLANT

(Plant I)

Particulate Size, microns	Cumulative Weight Percent Retained	
	Test No. 1	Test No. 2
>12.00	54.36	10.43
7.50	62.56	21.50
5.10	65.05	30.97
3.50	66.62	40.20
2.20	69.22	47.89
1.10	70.49	58.65
0.68	72.50	66.99
0.46	73.56	76.48
<0.46	100.00	100.00

Note: Particle size determinations were made with an Andersen Cascade Impactor.

Gaseous emissions obtained from the same tests are given in Table 6.[54]

TABLE 6. (PLANT I) GASEOUS EMISSIONS ENTERING THE ATMOSPHERE FROM AN ELECTROSTATIC PRECIPITATOR CONTROLLED SINTER PLANT

Gaseous Component	Milligrams / Nm^3	Grains / SCFD*	ppm
Condensable hydrocarbons	1.036	0.000453	-
Noncondensable hydrocarbons	812.11	0.3539	230
Fluoride	3.21	0.00140	-
Carbon monoxide	-	-	8000
Sulfur dioxide	-	-	900
Sulfur trioxide	-	-	11.5
Nitrogen oxides	-	-	71.4

*Standard cubic foot (dry).

For Plant I, particulate concentrations at the electrostatic precipitators were as follows:

	mg/m^3 (dry)	grains/ft^3 (dry)
Average ESP inlet	595	0.26
Average ESP outlet	69	0.03

This corresponds to a collection efficiency of 88.4 percent. Total emissions to the atmosphere amounted to 23.4 kg per hour (51.6 pounds per hour). This was equivalent to 0.214 kg per tonne (0.428 pound per net ton) of sinter.

V. RECLAMATION (SINTER) PLANT ELECTROSTATIC PRECIPITATOR DESIGN CHARACTERISTICS

This section of the report concerns design fundamentals for duct-type (i.e., those that use plates for collection), wet and dry electrostatic precipitators. Electrostatic precipitators using tubular or pipe collectors are not considered.

BASIC ELECTROSTATIC PRECIPITATOR PARTS*

The three basic parts of any precipitator installation are:

(1) Power supply
(2) Collection area
(3) Dust-removal area.

The power supply generally consists of a single-phase, high-voltage transformer, appropriate control equipment, and a bridge rectifier circuit. The rectifier circuit can be either a full-wave or double half-wave circuit, as shown in Figure 10.

Rectifier design has progressed from the mechanical rectifier to the high-voltage Kenotron vacuum tube, selenium, or silicon rectifiers. Normal transformer ratings are between 15 and 25-kva, 440-volt primary and 50 to 75-kv secondary. In order to limit short-circuit current surges, the transformer primary circuit usually contains a ballast resistance or a reactor. Manual or automatic control is used to regulate electrical conditions in the precipitator dust-collection area.

The collection area consists of duct collection electrodes with high-voltage discharge electrodes uniformly spaced and of uniform length,

*Reprinted from Iron and Steel Engineer, Electrostatic Precipitator Primer, J. Katz, by permission of the Association of Iron and Steel Engineers, pp. 21-40, May 1964.

Preceding page blank

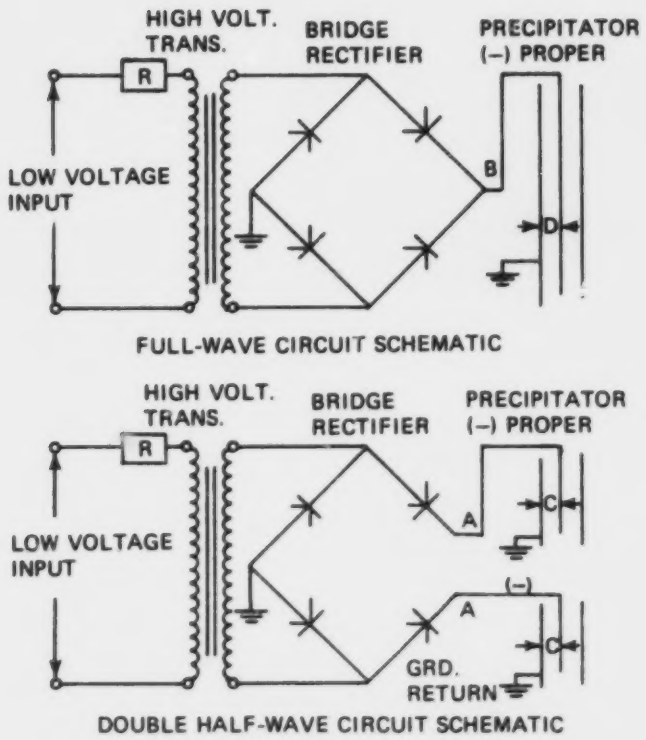

Figure 10. Two possible rectifier circuits for an electrostatic precipitator

as illustrated in Figure 11. Collecting electrodes (the metal surfaces that collect the particles) are at ground potential and are connected directly to the frame of the precipitator. The collecting-surface design varies with the manufacturing company and process. The duct collecting surface may consist of perforated or solid metal plates up to 6.1 x 1.4 meters (20 x 4-1/2 feet). Normally a precipitator has three to four duct sections in series. The duct width may be 200 mm (8 inches) although 250-mm (10-inch) ducts are sometimes employed in cleaning gases that contain large quantities of dust. There can be five or six discharge electrodes equally spaced in each 1.4-meter (4.5-foot) duct section. These discharge electrodes receive the high-voltage rectifier output and are suspended in parallel from a framework that is insulated from ground by ceramic insulators.

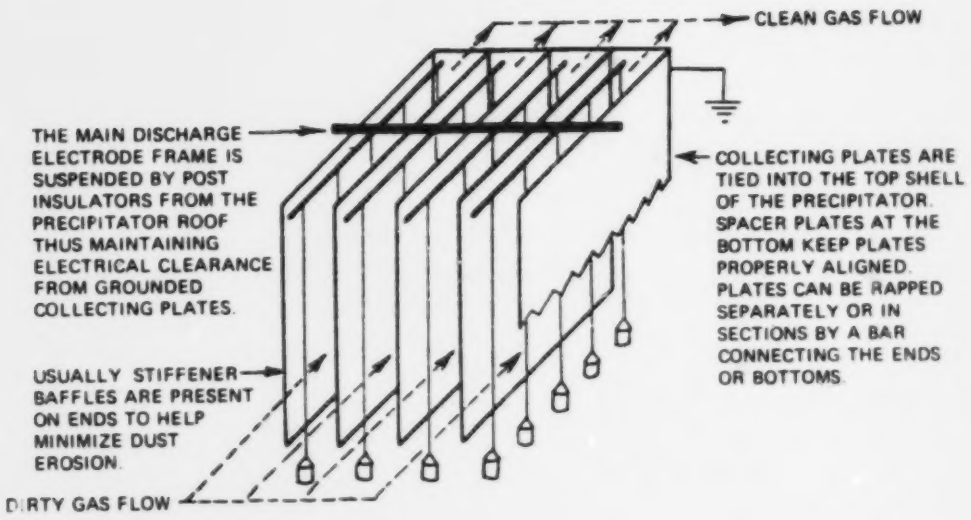
CLEAN GAS FLOW
THE MAIN DISCHARGE ELECTRODE FRAME IS SUSPENDED BY POST INSULATORS FROM THE PRECIPITATOR ROOF THUS MAINTAINING ELECTRICAL CLEARANCE FROM GROUNDED COLLECTING PLATES.
COLLECTING PLATES ARE TIED INTO THE TOP SHELL OF THE PRECIPITATOR. SPACER PLATES AT THE BOTTOM KEEP PLATES PROPERLY ALIGNED. PLATES CAN BE RAPPED SEPARATELY OR IN SECTIONS BY A BAR CONNECTING THE ENDS OR BOTTOMS.
USUALLY STIFFENER BAFFLES ARE PRESENT ON ENDS TO HELP MINIMIZE DUST EROSION.
DIRTY GAS FLOW

Figure 11. Typical duct electrostatic precipitator

Dust removal is accomplished either mechanically or hydraulically, depending on the physical state of the process. Most applications involve a dry process; the collected dust is removed by rapping or vibrating the plates. The method used to remove material from the collecting surfaces is most important to minimize particulate reentrainment and electrical disturbances. Material vibrated from the collecting plates falls into hoppers for subsequent removal.

Dry-Dust-Collection Fundamentals

Before discussing each of the major factors affecting the collection of particulates with electrostatic precipitators, it would be well to understand the process fundamentals. Simply stated, the process consists of charging dust particles with a corona discharge and then passing them through an electric field where they are attracted to the collecting surfaces.

There are five basic kinds of electrical discharge through a gas spacing between a high voltage circuit:

(1) The dark discharge is not visible although chemical action occurs. The current increases nearly linearly with voltage.

(2) The glow or corona is the most frequent initial discharge and is accompanied by a hissing noise. Current increases much faster than voltage.

(3) The brush discharge usually falls midway between corona and a spark. It consists of a number of small sparks ending in space and originates in surface irregularities or abnormalities in the conductors. Current increases with possibly a slight drop in voltage.

(4) The spark is a common discharge that is unstable in that the increased current lowers the voltage appreciably. It is the sudden rush of electric current through the gas, and is limited only by the circuit power supply. The spark is the most complete form of gas "breakdown".

(5) The arc is not ionization by collison as are the preceding four categories but arises from other discharges. Current density is very high, while the voltage decreases to a low value. This discharge is particularly unstable unless the current is limited by an external electrical circuit resistance.

In order for a current to flow across a gas space, ionization must be started and sustained by electron acceleration and collision with gas molecules causing a cumulative effect.

For the case of a negative wire in a cylinder, the following explanation describes the corona current ionization principle: Electrons are released from the wire surface by a positive-ion impact or photoelectric emission. These accelerating electrons in short movements near the wire surface generate new electrons and positive ions by molecular impact. The electrons quickly move away from the wire and attach to gas molecules to form negative ions or produce new

collisions. Once the corona glow begins, ultraviolet radiation may produce additional photoelectrons at the wire surface. As this electron collision continues, the negative ions build a dense cloud throughout the space between the active region near the wire and the passive anode. The effect of this ion space charge is to help limit the ionizing field near the discharge wire and also to stabilize the corona discharge.

This ion movement has two main charging effects on dust particles in the precipitator region between the electrodes.

(1) Suspended dust particles are bombarded toward the anode under the force of a strong electric field.

(2) Ion diffusion causes the negative ions to attach themselves to dust particles less than 0.2 micron in size and, by this method, transport these smaller particles to the collecting plate.

The following expresses the principles of the electron precipitator in theory.

Migration velocity or precipitation rate of particles:

$$\omega = \frac{a E_o E_p}{2 \pi \theta} \qquad (1)$$

where

a = particle radius, microns
E_p = strength of field in which particles are charged, statvolts/cm
E_o = strength of field in which particles are collected, statvolts/cm (normally the field close to the collecting plates)
θ = viscosity or frictional resistance coefficient of the gas, poises
π = 3.1416.

Collection efficiency of precipitator:

$$\eta = 1 - e^{-\left(\frac{A_c \omega}{V}\right)} \qquad (2)$$

where

A_c = effective collecting electrode area of the precipitator, sq m (sq ft)
V = gas flow rate through the precipitator, cu m per sec (cu ft per sec)
e = base of natural logarithms = 2.718
ω = migration velocity, m per sec (ft per sec).

The equation for efficiency is known as the Deutsch-Anderson equation.

Equation (1) shows that an increase in both particle size and electric fields, E_o and E_p, will increase precipitator performance, while increased gas viscosity will adversely affect performance. A study of Equation (2) shows that the precipitator efficiency increases with increasing values of the exponent $-A_c\omega/V$. Therefore, as the precipitator electrode area becomes greater and the migration velocity increases, precipitator performance improves. At the same time, if the gas flow rate increases, the precipitator performance decreases.

To illustrate the velocity with which a single dust particle moves to the collecting surface under the influence of an electric force, the following example is given for a typical steel-mill gas:

a = 1 micron particle = 10^{-4} cm
E_o = 4.8 kv/cm = 16 statvolts/cm
E_p = 6.0 kv/cm = 20 statvolts/cm
θ = 2.7×10^{-4} gas viscosity at 260 C (500 F), poises.

From Equation (1), the migration velocity is:

$$\omega = \frac{a\, E_o E_p}{2\, \pi\, \theta}$$

$$\omega = \frac{10^{-4} \times 16 \times 20}{2 \times 3.14 \times 2.7 \times 10^{-4}}$$

$$\omega = 18.9 \text{ cm/sec} = 0.62 \text{ ft/sec.}$$

If the discharging wire is 100 mm (4 inches) from the collecting plate and the gas flow through the duct is 1.22 m/sec (4 ft/sec), the dust particle would reach the collecting surface in approximately 0.6 meter (2 feet) of duct length.

Under similar dust and precipitator conditions but with the gas cooled to 150 C (300 F), the gas viscosity decreases to 2.3×10^{-4} poises:

$$\omega = \frac{10^{-4} \times 16 \times 20}{2 \times 3.14 \times 2.3 \times 10^{-4}}$$

$$\omega = 22.2 \text{ cm/sec} = 0.73 \text{ ft/sec.}$$

To determine the effect on conditions in the first example by increasing the average and peak precipitator voltages by 20 percent:

$$\omega = \frac{10^{-4} \times 19.2 \times 24}{2 \times 3.14 \times 2.7 \times 10^{-4}}$$

$$\omega = 27.2 \text{ cm/sec} = 0.9 \text{ ft/sec.}$$

The dust particle drift velocity to the collecting plate increased 50 percent when the precipitator voltages increased 20 percent.

Consider the first example except that the average dust particle size is now 5 microns:

$$\omega = \frac{5 \times 10^{-4} \times 16 \times 20}{2 \times 3.14 \times 2.7 \times 10^{-4}}$$

$$\omega = 95 \text{ cm/sec} = 3.1 \text{ ft/sec.}$$

Thus, a 5-micron particle should reach the collecting plate in about 0.43 feet of duct length with the 4-fps gas flow. When this is compared with the migration velocity of a 1-micron dust particle, it points up the need for an accurate dust-radius measurement to obtain the correct migration velocity for any gas.

To calculate a precipitator collection efficiency using an average dust particle size of 1-micron radius, substitute the original example migration velocity in Equation (2):

$$\eta = 1 - e^{-\left(\frac{0.189\, A_c}{V}\right)}.$$

A typical precipitator duct might have the following physical parameters:

Collecting surface A
= 6.2 m high x 3.6 m long x 2 sides = 44.6 sq m
= (20 ft high x 12 ft long x 2 sides = 480 sq ft).

Dust gas flow rate V at duct conditions
= 6.2 m high x 0.2 m wide x 1.22 m/sec = 1.51 cu m/sec
= (20 ft high x 0.667 ft [8-inch spacing] x 4 ft/sec = 53.4 cu ft/sec).

Substituting for A and V in Equation 2:

$$\eta = 1 - e^{-\frac{0.189 \times 45.1}{1.51}} = \left(1 - e^{-\frac{0.62 \times 480}{53.4}}\right)$$

$$\eta = 1 - 0.0037$$

$$\eta = 0.996 \text{ or } 99.6 \text{ percent.}$$

These equations help to explain precipitator performance scientifically. However, other factors result in discrepancies.

Factors Affecting Dry Electrostatic Precipitator Operation

The difficulties of dust adhering to the collecting plates, poor gas distribution and spark-over conditions are three factors that reduce the theoretical migration velocity. Each precipitator application will determine the deviation of the ω factor from field data. This provides a base for future installation calculations as well as a means for

comparing precipitators in the same application. The succeeding paragraphs will discuss the major factors that affect precipitation.

The migration velocity, ω, is quite sensitive to the voltage since the electric fields appear as a product in Equation 1. Therefore, the object is to obtain maximum voltage with proper corona current flow for maximum collection efficiency. The major factors that determine this condition are:

(1) Applied voltage frequency and waveform

(2) Spark-over characteristics

(3) Electrode characteristics

(4) Gas flow rate

(5) Gas flow distribution

(6) Dust concentration

(7) Dust composition, including particle size and resistivity

(8) Gas temperature, pressure and humidity.

Applied Voltage, Frequency and Waveform – The rectifier input is conventional 60-hertz power. Therefore, half-wave and full-wave energization contains 60 and 120 pulses/sec, respectively, as shown in Figure 12.

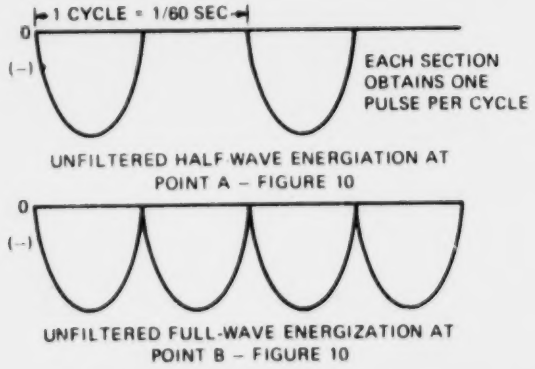
1 CYCLE = 1/60 SEC
0
(–)
EACH SECTION OBTAINS ONE PULSE PER CYCLE
UNFILTERED HALF WAVE ENERGIATION AT POINT A – FIGURE 10
0
(–)
UNFILTERED FULL-WAVE ENERGIZATION AT POINT B – FIGURE 10

Figure 12. Voltage waveform for unfiltered half-wave and full-wave rectification

Negative polarity is used. The negative wave is impressed on the discharge electrode while the grounded collecting electrode serves as the positive terminal. Negative polarity on the electron-emitting discharge wire has proved superior in that it allows a higher spark-over potential to be reached in the precipitator before a voltage breakdown occurs between the two electrodes.

Consider the precipitator proper as a number of parallel capacitors in which the high-voltage discharge electrode and the collecting electrode form the plates of the capacitor while the gas serves as the capacitor dielectric. Therefore, every voltage pulse tends to charge this precipitator capacitance, which provides a natural voltage filter as this capacitance discharges through the gas resistance, changing the actual precipitator voltage waveform to that of Figure 13. The maximum and minimum voltages are now simply E_p and E_m.

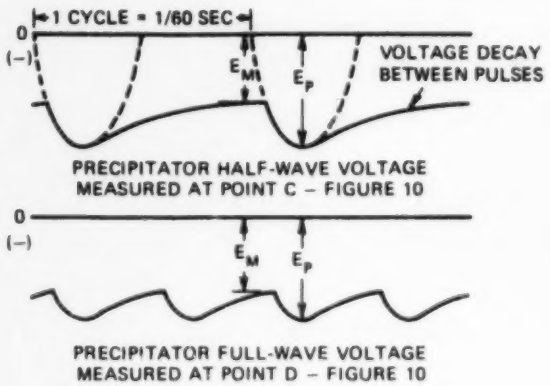

Figure 13. Waveform in electrostatic precipitator after discharge

The current output with half-wave energization is one-half that of full-wave energization. Also, the voltages E_p and E_m of the full-wave waveform are closer (i.e., the full-wave E_p is slightly less than the half-wave E_p), while the full-wave E_m is greater than the half-wave E_m. Half-wave energization has several advantages over full-wave in most installations.

Two of the major advantages are:

(1) The same rectifier output can be distributed to smaller precipitator areas, as shown in Figure 10. This construction necessitates additional switching and bus connections. However, the continuity of operation and collection efficiency will usually benefit from this construction since localized trouble in one section will not affect the electrical characteristics in other sections.

(2) The half-wave, because of the time lag between voltage pulses, is less likely to sustain a voltage breakdown between electrodes.

If, in Equation 1, E_o is the average field voltage, then $E_o = 1/2 (E_p + E_m)$. These measurements can be obtained by oscilloscope readings across appropriate voltage dividers. Typical field voltages in duct precipitators are:

E_p = 3.9 to 5.9 kv/cm (10 to 15 kv/in.)

E_m = 0.3 to 0.5 kv/cm (7 to 12 kv/in.).

Total corona current comprises a gas ionic current and a dust current in which electrons attach themselves to a dust particle. The ionic current is approximately 95 percent of this total current. Oscilloscope readings of current waveforms show that conductivity of an electron tube rectifier is in the range of 60 to 80 percent of each half cycle. The ratio of peak current to average current should be 4.0 to 5.0 for efficiency. The current will vary from 10 to 30 ma/100 sq m (1000 sq ft) of collecting area.

Alteration of the waveform by a pulse method of energization has definite potential advantages, but this technique has never been used commercially. Certainly, the adjustment of voltage, frequency, and waveform to fit individual precipitators could benefit efficiency, especially for high-sparking conditions between discharge wire and collection plate.

Spark-Over Characteristics – The voltage breakdown between electrodes for a given precipitator depends on many complex variables

and is the point of maximum power input. Field measurements have shown that under normal conditions, 50 to 100 voltage breakdowns (spark-overs) per minute are tolerable. On the basis of half-wave energization with a possible 3600 pulses per minute, additional power input can be obtained with 100 sparks per minute since the voltage collapse during the spark-over is more than offset by the higher input during the nonsparking cycle. One must differentiate between spark-over and a power arc in that a spark-over is 1/2-cycle duration or less while a power arc may last several cycles and is quite detrimental to precipitator performance. Some precipitator applications will not spark within power-supply input limitations because of dust and gas conditioning. In most cases, the quantity of water carried by the gases and the gas temperature play an important part in this phenomenon.

Electrode Characteristics – Electrode configuration determines voltage and current characteristics. Diameter and shape of the discharge electrode determines the initial voltage required to start a corona discharge. For most practical gas applications, this voltage varies from 16 to 26 kv. In addition to material strength, two important factors that affect the operation of the discharge electrode are the wire diameter and curvature of the corona-emitting surface. The smaller the wire diameter, the greater is the corona current for any given voltage. The spacing between the discharge wire and collecting surface determines the required voltage. If the discharge wire is not centered perfectly within the collecting area, the spark-over voltage is reduced. Higher stress concentration exists in the reduced clearance between the wire and collecting electrode. This phenomenon of concentration points becomes very important with some types of collecting surfaces. Surface imperfections and slight differences in collection-plate construction can reduce spark-over voltage. Figure 14 shows the relationship between field voltage and collection efficiency and illustrates the importance of providing maximum field voltage. Imperfections or stress concentrations in electrode design should be minimized, especially with dusts resistive to current. The solid collecting plate is a recent design that minimizes spark-over between electrodes. Dust buildup on the discharge electrode, by producing a change in electrode configuration, can cause stress concentrations at the bottom and the top of the dust deposit. Dust buildup on the discharge wire tends to reduce corona current. The close spacing between discharge wires can also result in current reduction.

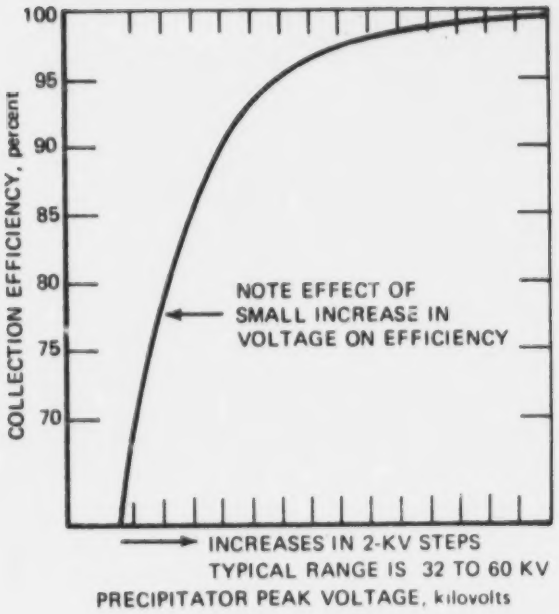

Figure 14. Dust-collection efficiency as related to peak voltage for a typical electrostatic precipitator

Changing the wire-to-wire spacing alters current-voltage relationships. When the discharge wires are relatively far apart, the current per unit length of wire tends to remain constant. As the wires are spaced closer and closer, the starting voltage increases, which tends to lower the current. Therefore, there is an optimum wire-to-wire spacing for which the total current is a maximum, and practice indicates that this spacing should be 150 percent of wire-to-plate spacing. An interesting aspect of wire-to-wire spacing is that the field strength near the plate is less midway between wires than it is directly opposite the wires. Therefore, the closer the discharge wires are to each other, the higher the average field strength until the current is suppressed.

The corona current also depends on the wire-to-plate spacing and changes inversely as the square of the ratio between two different spacings. If the wire-to-plate spacings were reduced from 100 to 75 mm (4 to 3 inches), the corona current would practically double.

However, if the wire spacing were increased from 100 to 125 mm (4 to 5 inches), the corona current would decrease about one third.

Gas Flow Rate – Collection efficiency of the precipitator is designed on a gas-volume basis. However, the effect of gas flow on performance is sensitive to several factors:

(1) In a high-sparking unit where power input must be less than required to reach the designed collection efficiency, improved collection can be obtained at 70 to 80 percent of precipitator gas-volume rating. Actually, a distinct difference in performance will be noted under these conditions, as illustrated in Figure 15.

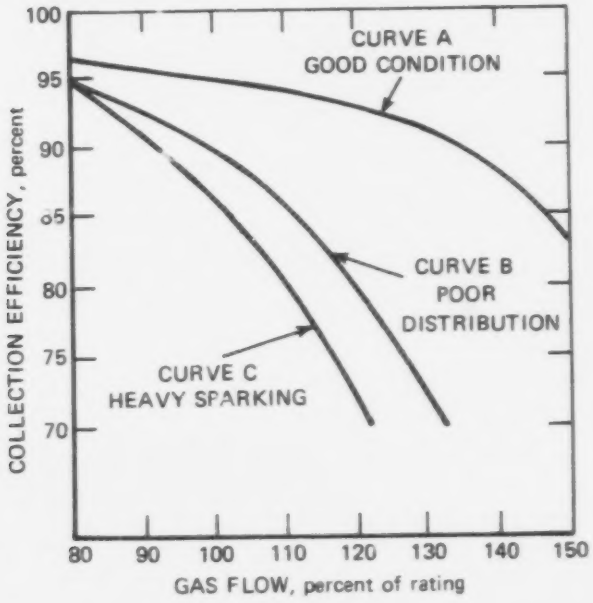

Figure 15. Electrostatic precipitator efficiency as affected by gas flow

(2) With maximum voltage fields and power input, gas volume overloads of 10 to 25 percent have little effect on collection efficiency. In fact, the dust size determines just how much excess volume is possible, since reentrainment in the gas is greater with large-dust-particle collection and is minimized with fume and wet collection. Migration drift velocity is greatest with maximum voltage which can overcome gas flows of even 4.6 m/sec (15 ft/sec) through collecting areas of some cleaning applications.

Gas Flow Distribution – Precipitator performance may deviate from design calculations because of poor gas distribution through the precipitator inlet. Consider an installation designed for 95 percent collection efficiency where one-half the precipitator is treating 75 percent of the gas volume. Depending on the dust, a 5 to 20 percent decrease in collection efficiency may result. This condition is the same as overloading the one half of the precipitator with 150 percent of rated gas volume.

In an inlet cross section composed of 20 to 30 equal areas, the designer should assure that no single area deviates more than 10 to 15 percent from the average cross-sectional flow. It is important that minimum gas turbulence coincide with the optimum gas pattern. Minimum gas turbulence is a direct function of inlet flue design and gas flow directing vanes and baffles if used. Usually the gas flow from a particular process travels at high velocities (from 9.1 to 18.3 m/sec (30 to 60 ft/sec) and must be reduced to 1.5 to 3.0 m/sec (5 to 10 ft/sec) at the precipitator inlet. Careful study at this stage of the design can often insure a highly efficient unit. If the size of the installation or critical nature of the process warrants the additional cost, gas-flow pattern can be investigated in scaled-down glass models of the proposed structures. However, duplicating actual gas-flow conditions in glass-model studies presents many problems.

To help reduce gas turbulence and poor distribution, low-pressure-drop plates across the precipitator inlet are normally employed. However, a low-pressure drop across these plates may not drastically alter existing conditions. After the unit goes into operation, it is wise to measure the distribution pattern across the inlet with a pitot tube or other suitable means. Field alterations can be made on the basis of actual measured results.

The kind of dust collected by the precipitator influences the effect of gas distribution on precipitator efficiency. In most cases, fumes or fine dust have less effect than gases containing larger dust particles. In the last analysis, poor gas distribution reduces collection efficiency appreciably since it adversely affects the electrical characteristics. The power input of a precipitator section is limited by the lowest spark-over point of that section.

Dust Concentration – An interesting facet of electrostatic precipitation is the effect that the quantity of dust has on the cleaning process. The dust concentration does not basically influence the precipitator's size for any given efficiency. The following facts should be considered when dust concentrations are heavy. First, the quantity of dust alters voltage-current characteristics: more dust increases voltage and reduces current. Second, frequent dust removal from the collecting electrode should minimize dust reentrainment in the gas stream. Third, if the dust quantity is great enough, the first section may require 254-mm-wide (10-inch-wide) ducts to eliminate a possible spark-over caused by excessive voltage buildup.

If the dust is discharged to the atmosphere, the dust quantity must meet minimum stack discharge specified by community air-pollution ordinances. Considering two different gas concentrations of 2.3 and 34 grams/cu m (1.0 and 15 grains/std cu ft) flowing through a 95 percent efficient precipitator, comparative outlet dust discharges would be as follows:

$$(2.3 \text{ grams/cu m}) \times (1.0-0.95) = 0.12 \text{ gram/cu m}$$
$$(34.0 \text{ grams/cu m}) \times (1.0-0.95) = 1.70 \text{ grams/cu m}$$

$$(1.0 \text{ grains/std cu ft}) \times (1.0-0.95) = 0.05 \text{ grain/std cu ft}$$
$$(15.0 \text{ grains/std cu ft}) \times (1.0-0.95) = 0.75 \text{ grain/std cu ft.}$$

In order to obtain an outlet discharge of 0.12 gram/cu m (0.5 grain/std cu ft) with an inlet concentration of 34 grams/cu m (15 grains/std cu ft) the following precipitator efficiency is required:

$$\left(1.0 - \frac{0.12 \text{ gram/cu m}}{34.0 \text{ grams/cu m}}\right) 100 = 99.67 \text{ percent}$$

$$\left(1.0 - \frac{0.05 \text{ grain/std cu ft}}{15.0 \text{ grains/std cu ft}}\right) 100 = 99.67 \text{ percent} .$$

This efficiency can be obtained with the electrostatic precipitator but the process should warrant the additional cost of carefully optimizing the design.

Typical dust concentrations in iron and steel industry waste gases are:

Open-hearth furnace – 0.12 to 3.43 grams/cu m (0.05 to 1.5 grains/std cu ft)

Basic blast furnace after usual primary dust collection – 9 to 11 grams/cu m (4.0 to 5.0 grains/std cu ft)

Oxygen steelmaking furnace – 9 to 21 grams/cu m (4.0 to 9.0 grains/std cu ft) average

Ferromanganese blast furnace after primary dust collection – 23 to 34 grams/cu m (10.0 to 15.0 grains/std cu ft).

Particle Size and Resistivity – The migration velocity is directly affected by dust-particle size as noted in the basic formula. Small particles are more difficult to precipitate out of the gas stream than large particles, and require higher power and voltage to remove. Although the coarser particle is more easily collected, it may also be more easily lost to the gas stream through reentrainment resulting from vibration of the collection plate or erosion caused by gas eddy currents.

This lack of dust adhesion is a major factor in reducing the actual precipitator efficiency below a value predicated by the calculated migration velocity. For example, although the large particle does reach the collecting plate in a shorter time, reentrainment in the gas stream can take place throughout the length of the precipitator until, finally, the particle is lost to the atmosphere. The coarse or large particle is important in some applications in that it may keep the submicron dust from impacting on the collecting plate.

Particle size in waste gases from open-hearth processes will generally vary from <0.5 to 5 microns, and from 15 to 25 microns and larger from sintering-plant operations. The smaller particles of ferrous oxide come from open-hearth, electric-furnace, and oxygen-vessel fumes. Submicron particles are difficult to precipitate and have a tendency to suppress corona current if numerous enough. This characteristic is similar to the space charge around a discharge electrode. Voltage-current relationship is marked by high precipitator voltage and practically nil corona current. Although high-voltage fields are desirable, the electrostatic collecting process still requires sufficient corona current to sustain ionic movement to the collecting plates.

Another interesting effect of dust-particle size is the influence on visual stack discharge. The finer particles cause the stack discharge

to appear quite dense, while the actual weight of dust in a given volume of gas could fall well within air-pollution ordinance requirements. This phenomenon, caused by the greater surface area of submicron particles per unit weight, is significant not only from a community goodwill standpoint, but more importantly because of the fact that the emissions are respirable particles.

In previous paragraphs, maximum power input and high-voltage fields were prerequisites for efficient performance. Although the several factors discussed earlier will tend to lower spark-over voltages, the optimum electrical characteristics depend primarily on the resistivity of the particular dust. In other words, will the dust resist or will it react favorably to the corona current flow?

High-resistivity dust causes severe sparking between electrodes so the power input must be reduced to reach the desirable spark-over rate of 50 to 100 sparks per minute. Under these conditions, precipitator performance sometimes runs 5 to 20 percent below design values. The chemical composition of the dust particle directly affects its electrical characteristics. However, proper gas temperature and humidity can alter the dust-resistivity range to obtain good results. In some cases, additional water, steam, or a special conditioning gas can be injected into the gas stream to realize optimum electrical results.

With the wet process of removing deposits from collecting surfaces, excessive spark-over because of dust resistivity is insignificant. Where a highly resistive dust is deposited on dry collecting surfaces, a voltage gradient across the dust layer can be high enough to emit its own corona discharge. This situation can disturb electrical conditions, with excessive sparking at lowered voltages or with excessive current at greatly lowered voltages without sparking. This second condition can produce enough positive ions to counteract the negative space charge and significantly reduce the migration rate. The term back-discharge or back-corona commonly describes this situation. Low gas moisture content with the absence of certain chemical impurities in the temperature range 116 to 232 C (240 to 450 F) is likely to cause a highly resistive dust condition.

Temperature, Pressure, and Humidity – In any particular precipitator installation, varying temperature, pressure, or humidity will cause some change in electrical characteristics. Since higher gas

temperature will decrease gas density, lower precipitator voltages and higher currents are usually obtained. Higher gas pressure will have an opposite effect by increasing the voltage and decreasing the corona current. This phenomenon parallels the effect that increased dust concentration has on corona power. In addition, if a highly resistive dust is encountered, the resistivity can be varied by either increasing or decreasing gas temperature from a maximum resistivity operating range. This maximum resistivity will vary with the kind of dust, but the band width will normally encompass 50 to 80 C (90 to 150 F) as illustrated in Figure 16.

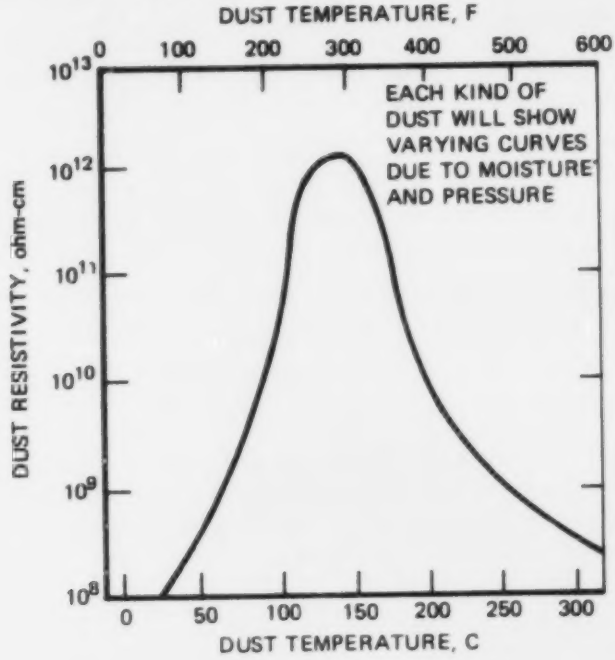

Figure 16. A typical relationship between dust resistivity and temperature for a gas improperly conditioned for the 93 to 204 C (200 to 400 F) range

Moisture affects the electrical conditions indirectly and directly. Moisture indirectly decreases dust resistivity, while it directly increases the spark-over voltage appreciably. In the gas-temperature range below 260 C (500 F), the indirect and direct effects from the addition of moisture are equally beneficial. Over 260 C (500 F), the direct effect of raising the spark-over voltage predominates.

Increasing the moisture content usually produces a rise in precipitator voltage and a drop in current.

Dust Removal From Collection Plates – One factor not included in the fundamental precipitation formula but of major practical concern is the vibration or rapping method employed to remove dust buildup from electrode surfaces. Various equipment and methods are available but all should

(1) Minimize irregular dust buildup on electrode surfaces to reduce spark-over possibilities

(2) Offer rapping cycles of short enough duration to eliminate dust puffs through the stack

(3) Determine the type of rapping system, whether vibrating or single blow, that provides optimum dust removal with special dust composition, temperature, and humidity conditions

(4) Design the collecting area controlled by each plate rapping system as small as economically possible

(5) Provide for varying the rapping magnitude between inlet and outlet precipitator sections

(6) Above all, the pattern of any rapping system should be determined from internal inspection if poor precipitator performance is attributed to inefficient rapping.

Dry Electrostatic Precipitator Design Methods

The two methods used in the design of all electrostatic precipitators both rely on empirical relationships developed by equipment manufacturers over their years of construction experience. The first method is based on the conventional Deutsch-Anderson efficiency equation and the second method approaches the design from the standpoint of the electrical requirements. These methods must obviously give compatible results. They differ mainly in the fundamental way in which design is approached.

Dry Electrostatic Precipitator Design Method I – A common approach to the selection of the area of collecting plate required is to utilize the Deutsch-Anderson equation

$$\eta = 1 - e^{-\left(\frac{A_c \omega}{V}\right)}$$

where

η = efficiency
A_c = effective electrode collecting area, sq cm (sq ft)
V = gas flow rate through the precipitator, cu cm/sec (cu ft/sec)
ω = migration velocity, cm/sec (ft/sec) (precipitation-rate parameter)
e = base of natural logarithms = 2.718.

The critical parameter in this equation is the precipitation rate ω. This parameter varies with each installation, depending upon resistivity and particle size of the dust, quality of gas flow, reentrainment losses, and sectionalization, among other factors. The values of ω are selected by the equipment manufacturers on the basis of past experience with a particular dust, or from the composition of the dust that can be related to past experience. Each precipitator manufacturer therefore has a file of experience from which a precipitation rate parameter can be selected, and this file of information is kept as proprietary data.

The values of the precipitation-rate parameter ω vary with the application as a result of variations in dust properties. Variations also occur within each application area. Table 7 lists the average values of precipitation-rate parameter for various applications, and the range of values that might be expected within each application. From this table, it is apparent that the spread in the values of the precipitation-rate parameter is large in some instances, such as in fly-ash precipitators, and within a reasonably narrow range in others.

The major problem in the design of precipitators based on this approach is the selection of the precipitation-rate parameter for the specific application. Several techniques can be used to narrow the uncertainty of the value of ω to be used. If the in situ resistivity of dust is known, the precipitation-rate parameter can be determined for some applications. Figure 17 shows the variation in ω with

TABLE 7. REPRESENTATIVE PRECIPITATION RATES, ω, FOR VARIOUS APPLICATIONS

Application	Average		Range	
	cm/sec	ft/sec	cm/sec	ft/sec
Utility fly ash	13.1	0.43	4.0-28.4	0.13-0.67
Pulp and paper	7.6	0.25	6.4- 9.5	0.21-0.31
Sulfuric acid	6.3	0.24	6.1- 8.6	0.20-0.28
Cement (wet)	10.7	9.35	0.3-12.4	0.30-0.40
Smelter	1.8	0.06	n.a.	n.a.
Open hearth	4.9	0.16	n.a.	n.a.
Cupola	3.1	0.10	n.a.	n.a.
Blast furnace	10.9	0.36	6.1-14.0	0.20-0.46
Sinter plant	n.a.	n.a.	2.3-11.5	0.07-0.38

n.a. – data not available.

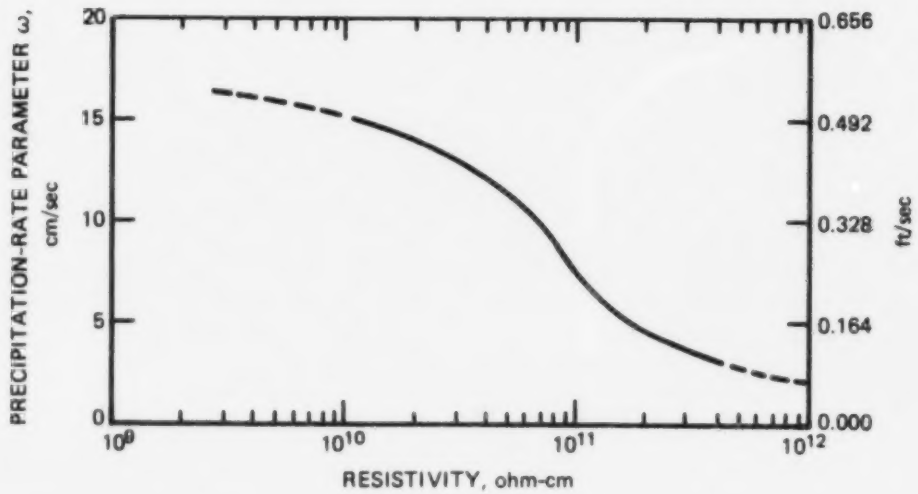

Figure 17. Relationship between precipitation-rate parameter ω and resistivity of fly ash

resistivity for fly-ash precipitators. If the precipitator being designed is a replacement for, or an addition to an existing unit, resistivity can be measured, and the uncertainty in the value of ω can be reduced. Alternatively, if a similar installation is available, measurements of resistivity can be made and the value of ω selected with some confidence.

The data from Figure 17 apply only to fly ash or to a dust with similar properties. If the particle size differs significantly, the absolute values of ω will change, although the general character of the curves would be similar.

In situ resistivity data have not been determined to the same degree in applications other than in fly ash precipitators, so that statistically reliable data relating ω and resistivity are not generally available.

If it is impractical to select ω on the basis of resistivity, other factors can often be used. In fly-ash precipitators, resistivity is influenced by the sulfur content of the fuel, and relationships have been developed between precipitation-rate parameter ω and percentage of sulfur content. Figure 18 shows a curve developed for a group of fly-ash precipitators burning coals with varying sulfur contents. On a statistical basis, the precipitation rate can be predicted within reasonable accuracy. However, on an individual installation, the variations are too great to predict ω with acceptable precision on the basis of sulfur content alone. In many instances, the only information available is the sulfur content of the coal, and designs are sometimes based solely upon this parameter.

Particle size of the dust is a very important consideration in determining the value of ω for design purposes. Referring to Table 5, the variations in ω between the various application areas are due largely to particle-size variations. In cement kilns, the alkali content of the raw material alters the size distribution of the dust. Metallurgical operations characteristically produce smaller size dusts from high-temperature melting operations. Size of dusts from recovery boilers in pulp and paper mills can change with temperature. These factors result in variations in precipitation-rate parameters between the various applications, and within the same application area.

When the selection of precipitation-rate parameter has been made, the area of collecting surface required to achieve a given efficiency when handling a given gas volume can be determined.

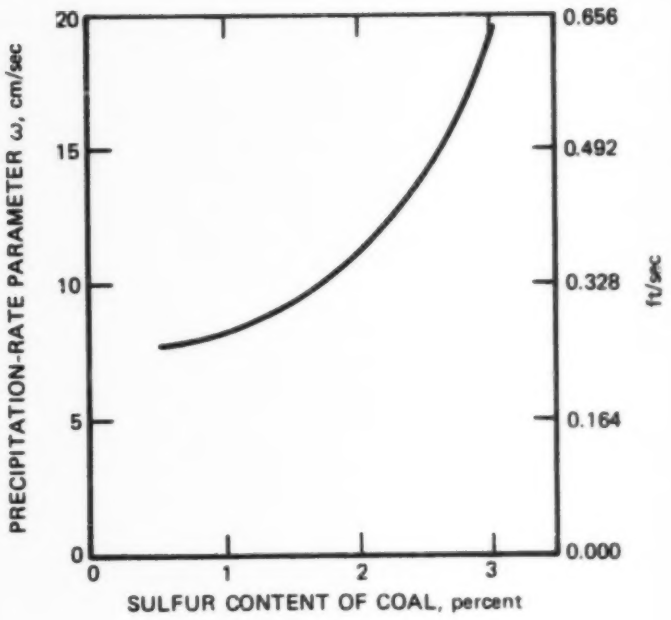

Figure 18. Relationship between the sulfur content in electric utility plant fuel and the precipitation-rate parameter ω at 149 C (300 F)

The power required for a particular application is determined on an empirical basis. The power requirements for a given application are related to the efficiency and the gas volume handled. Figure 19 is a curve showing the power requirements per unit of gas volume for two applications: fly-ash precipitation and pulp- and paper-mill recovery boiler precipitation. Similar curves can be developed for other applications. The second step in design, therefore, is to determine the total power requirements based on efficiency and gas flow. Note that the recovery-boiler precipitators require greater power per unit of gas flow to achieve the same efficiency as that of a fly-ash precipitator. This is primarily due to differences in particle size of the dust and is related to the precipitation-rate parameter.

Figure 20 shows the variation in collection efficiency with the number of independently powered bus sections. The number of sections required to reach a given efficiency can be determined from curves

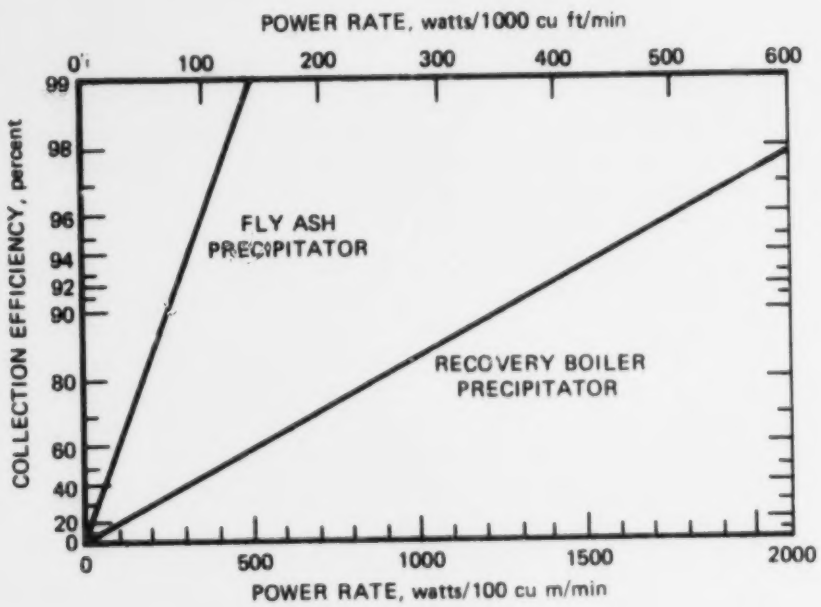

Figure 19. Collection efficiency as affected by power rate per unit gas flow

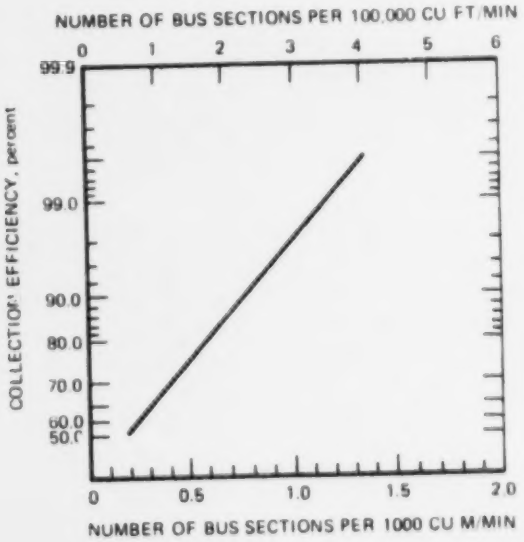

Figure 20. Relationship between collection efficiency and sectionalization (number of bus sections per unit gas flow) for utility fly-ash precipitators

for the specific application. The relationship shown in Figure 21 is for fly-ash precipitators and was developed from empirical relationships from a large number of tests.

The above procedure will provide a rational basis for arriving at plate area, total power, and degree of sectionalization required. It should be recognized that the selection of the value of ω and the curves relating power and sectionalization requirements are all interrelated. If inadequate sectionalization is used, a lower value of ω would result, the precipitator could not be operated at the required power level, and the efficiency would be reduced. Consequently, curves relating the design parameter should be internally consistent.

The type and number of rappers for the collecting and discharge electrodes depend upon the properties of the dust, gas properties, current densities, and the configuration of the electrodes and electrode support structures. High-resistivity dust is usually harder to remove because of the increased force holding it to the plate. Low-temperature operation also tends to give a moist dust that is more difficult to remove. Table 8 shows the number of rappers per unit are of collecting electrode and the number per unit length of discharge wire for a group of installations.

TABLE 8. NUMBER OF RAPPERS IN ELECTROSTATIC PRECIPITATORS FOR VARIOUS APPLICATIONS

	Collection Electrode		Corona Electrode	
Application	Number Rappers 100 Square Meters	Number Rappers 1000 Square Feet	Number Rappers 100 Meters	Number Rappers 1000 Feet
Utilities	0.27-0.97	0.25-0.90	0.03-0.22	0.09-0.66
Pulp and paper	0.27-1.07	0.25-0.99	0.07-0.10	0.21-0.32
Metals	0.12-0.88	0.11-0.82	0.09-0.16	0.28-0.50
Cement	0.35-0.56	0.33-0.52	0.06-0.11	0.19-0.33

The following example will serve to illustrate this design approach. Design an electrostatic precipitator for a pulverized fuel boiler with the following given conditions:

(1) Dust resistivity, 7×10^{10} ohm-cm

(2) Gas temperature, 149 C (300 F)

(3) Gas volume, 21,240 actual cu m/min (750,000 actual cu ft/min)

(4) Sulfur content, 1.8 percent

(5) Efficiency, 99 percent.

Example:

(a) Select a precipitation-rate parameter.
From Figure 17 the precipitation-rate parameter corresponding to a dust resistivity of 7×10^{10} ohm-cm is about 10.7 cm/sec or 6.4 m/min (0.35 ft/sec or 21.0 ft/min)

(b) From the Deutsch-Anderson equation

$$\eta = 1 - e^{-\left(\frac{A_c \omega}{V}\right)}$$

or rearranging

$$A_c = \frac{V}{\omega} \ln \frac{100}{100 - \eta}$$

$$A_c = \frac{21,240}{6.4} \ln \frac{100}{100 - 99} \qquad A_c = \frac{750,000}{21} \ln \frac{100}{100 - 99}$$

$$= 3319 \ln 100 \qquad = 35,700 \ln 100$$

$$= 15,285 \text{ sq m} \qquad = 164,000 \text{ ft}^2.$$

(c) Compute total power requirements.
From Figure 19, power required for 99 percent efficiency is 495 watts/100 cu m/min (140 watts/1000 cu ft/min).

For 21,240 cu m/min (750,000 cu ft/min), total power = 212.4 x 495 = 105,000 watts (750 x 140 = 105,000 watts).

(d) Determine number of bus sections.
From Figure 20, number of bus sections required is 1.22/1000 cu m/min (3.5/100,000 cu ft/min).

21.24 cu m/min x 1.22 = 26 bus sections (7.5 cu ft/min x 3.5 = 26 bus sections).

(e) Determine the number of rappers required on the basis of past experience (see Table 8).

Dry Electrostatic Precipitator Design Method II - A second approach to the sizing of precipitators is to determine the electrical characteristics first and then develop relationships that relate efficiency and power requirements to the required collection-surface area. The concept of the electrical approach is based on the theoretical factors that influence the precipitation-rate parameter, that is, the current required to charge the particles and provide the space charge field, and the voltage required to establish the electrostatic collection field.

In this design method, the curves relating efficiency and corona power density are developed on an empirical basis. The curves are the same as that for Design Method I, and are given for fly ash and recovery boiler precipitators in Figure 19. Figure 21 is an empirically developed curve showing relationship between precipitation-rate parameter

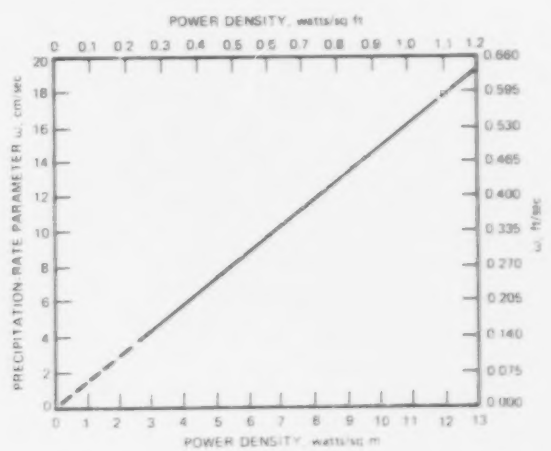

Figure 21. Relationship between precipitation-rate parameter ω and power density for fly ash precipitators

ω and corona power density. Since the total power has been determined previously, the collecting surface area can be computed from the data read from Figure 21. The number of independent bus sections can be determined in the same manner as in Method I. The following example will serve to illustrate the design procedure based on this method.

Example:

(a) Select a precipitation-rate parameter.
From experience with this coal, the precipitation rate parameter is selected to be 10.7 cm/sec (0.35 ft/sec).

(b) Compute corona power.
From Figure 19, power per unit volume corresponding to a collection efficiency of 99 percent is 495 watts/100 cu m/min (140 watts/1000 cu ft/min).

The total power is then computed:

$$P = \frac{495 \text{ watts}}{100 \text{ cu m/min}} \times 21,240 \text{ cu m/min} = 105,000 \text{ watts.}$$

$$P = \frac{140 \text{ watts}}{1000 \text{ cu ft/min}} \times 750,000 \text{ cu ft/min} = 105,000 \text{ watts.}$$

(c) Determine collection electrode area.
From Figure 21, for ω = 10.7 cm/sec (0.35 ft/sec), power density = 6.89 watts/sq m (0.64 watts/sq ft).

$$\text{Collection electrode area} = 105,000 \text{ watts} \times \frac{\text{sq m}}{6.89 \text{ watts}}$$
$$= 15,240 \text{ sq m}$$

$$\text{Collection electrode area} = 105,000 \text{ watts} \times \frac{\text{sq ft}}{0.64 \text{ watts}}$$
$$= 164,000 \text{ sq ft}$$

(d) Number of electrical sections.
From Figure 20, the number of sections per 1000 cu m/min at 99 percent efficiency = 1.22 (sections per 100,000 cu ft/min = 3.5).

$$\text{Number of sections} = \frac{1.22}{1000 \text{ cu m/min}} \times 21,240 \text{ cu m/min}$$
$$= 26.$$

$$\text{Number of sections} = \frac{3.5}{100,000 \text{ cu ft/min}} \times 750,000 \text{ cu ft/min}$$
$$= 26.$$

It should be noted that the curves relating the various factors in Method II must also be mutually compatible. The major difference between these two design methods is that the empirical data are used to arrive at the collecting-surface area as opposed to the use of the Deutsch-Anderson equation. In the examples shown, the precipitation-rate parameter ω was used in both instances. However, it is possible to develop other relationships that would eliminate the necessity for arriving at a value of ω altogether. Such relationships would be empirical and would be subject to the same degree of uncertainty as the selection of the precipitation-rate parameter.

A more fundamental approach to precipitator design would be that based upon theoretical factors such as particle size, gas composition, dust resistivity, precipitator dimensions, and other input conditions. This method is discussed in the following section. However, at this time, techniques for design based only on theoretical relationships have not been developed to the extent that they can be used on a commercial basis.

WET ELECTROSTATIC PRECIPITATOR

The use of wet electrostatic precipitators for control of emissions from industrial sources was generally restricted to rather specialized applications such as on acid mist, coke-oven off-gas, blast furnaces, and detarring applications. The method of cleaning was in most cases intermittent and of the wetted-wall type.

As a result of much more stringent local, state, and federal emission regulations, condensable materials were added to the total particulate loading. The removal of organic condensables, which are very difficult to wet and which form small droplets in the 0.1 to 2-micron range, requires scrubber pressure drops in the range from 100 to 150 cm (40 to 60 inches) of water gage. Since the wet electrostatic precipitator is always operated at saturation temperature (100 percent relative humidity), it will remove organic materials with a condensation temperature higher than or equal to the gas saturation temperature. It will also remove solid dust particles in the submicron range and gaseous contaminants soluble in the spraying liquor. The removal of emissions is done with very low energy consumption and a pressure drop usually less than 12.7 mm (0.5 inch) of water gage. The electric power input through the high-voltage power supplies is quite low, from 1.8 to 2.8 kw per 100 actual cu m/min (0.5 to 0.8 kw per 1000 actual cu ft/min).

The recent development of a continuously sprayed, parallel plate, frame electrode and horizontal flow design has provided industry with a realistic alternative to high-energy scrubbers. The theory of operation, description of the design, range of applications, limitations of the method for performance prediction, and the energy consumption are discussed in the following sections.

Wet-Dust-Collection Fundamentals[55]

The corona generation and the charging and discharging processes in the wet electrostatic precipitator are, in general terms, similar to what takes place in a conventional dry electrostatic precipitator except for some important differences.

Since the gas in the wet precipitator is always saturated with water vapor, there the current and voltage relationship is somewhat different from that in the dry precipitator. With increasing amounts of water vapor, the spark-over voltage increases (i.e., the voltage at which the field breaks down), but the corona current at a given voltage is lower. When solid particles and droplets enter the electrostatic field, they will cause a local distortion of the electrostatic field between the electrode and the collecting plate. Some of the electric-field lines intersect the particles, and ions generated by the corona discharge will tend to travel along lines of maximum voltage gradient or along the field lines; therefore, some of the ions will collide with the particles and the charge gradually builds up on the particles.

This process continues until the charge on the particles is so high that it diverts the electric-field lines away from the charged particles, preventing new ions from colliding with the dust particle. When this state has been reached, the particles are said to be saturated with charge. Theory shows that the saturation charge value and charging time are dependent upon electric-field strength, size of the particle, the dielectric constant of the particle, and the relative position of the particle in the field. This charging process is said to be field dependent and is the dominant process down to a particle size of 0.2 μm. For smaller particles, the so-called diffusion charging process is the dominant mechanism; this is governed by the random thermal motion of the ions and is not limited to a saturation charge.

As soon as the charging process of the particle starts, the resulting electrostatic force will pull the particle towards the collecting plate. This force, together with the gravitational and the drag forces, and the gas flow distribution in the field determine the particle trajectory and its point of collection.

In a dry electrostatic precipitator, the dust buildup on the collecting plate limits the maximum voltage at which the precipitator can operate. For dust layers with high resistivity (greater than 2×10^{10} ohm-cm) the voltage drop can be from 10 to 20 kv. This condition lowers the field strength in the space between the electrode and the dust deposit surface, and results in a lower saturation charge, which again gives a lower electrostatic force. If, on the other hand, the resistivity of the dust layer is lower than 10^7 ohm-cm, the electrostatic force holding the dust particle on the plates is low, and reentrainment can become a serious problem during the electrode and plate cleaning (rapping) cycle and also during the steady operation, having the overall effect of lowering the precipitator collection efficiency.

For a continuously sprayed wet electrostatic precipitator, the previously discussed problems are nonexistent. The spray liquid drops form a film on the collecting plates which continuously washes off the dust that is being collected; the resistivity of the liquid film is the governing factor in the dust-discharging process and not the resistivity of the dust layer itself. Reentrainment problems are also nonexistent, since the collected particles are instantaneously and continuously removed from the point of collection and are washed down as a light slurry. The exit loading is, therefore, much more stable and does not have the characteristic sharp increase that the dry electrostatic precipitator has during the collection plate and electrode rapping cycles.

Therefore, for a wet electrostatic precipitator, the operation is not influenced by the resistivity of the dust layer. The major parameters that must be considered are the particles' dielectric constant and size.

In order to better understand the effect of low dielectric constants on horizontal migration distance of the particle, a mathematical model of the particle collection mechanism was developed. The analysis was based upon a field charging process and a particle or droplet which had to traverse the whole net field spacing (one half of the plate-to-plate spacing). Particles of different sizes with dielectric constants of 2, 10, and 78 were investigated.

The unit consisted of parallel collecting plates with a separation of 2r. The velocity profile between the plates was assumed to be flat (plug flow) and turbulent drag forces were neglected. Centered between two plates was an electrode frame, with electrode spacing assumed sufficiently close to provide an approximately uniform electrostatic field near the plate surface. The field strength was approximately 70 percent of the field that was to be produced by a solid discharge plate electrode, or

$$E = -0.70\, dv/dr. \tag{3}$$

The nomenclature for the equations is given in Table 9.

The current density under no-load condition will be

$$J = i/A_c. \tag{4}$$

The ionic space charge can be determined from the current density – electric field equation:

$$J = N_o e \mu_i \overline{E} \quad (\overline{E} = \text{mean electrostatic field strength}). \tag{5}$$

TABLE 9. NOMENCLATURE FOR WET-DUST-COLLECTION FUNDAMENTALS

A	=	$6\pi a\eta/m$ = constant
A_c	=	Collection area
a_d	=	Particle diameter
B	=	$q_s E/m$ = constant
c_i	=	Particle inlet loading
c_o	=	Particle outlet loading
E	=	Electrostatic field strength
e	=	Electric charge
F	=	Force
g	=	Gravitational constant
i	=	Current
J	=	Current density
ln	=	Natural logarithm
m	=	Particle mass
N_o	=	Number density of free ions
V	=	Gas flow rate
q	=	Charge
q_s	=	Saturation charge
r	=	Net field spacing
s_x	=	Transverse distance
s_z	=	Horizontal distance
T	=	Migration time for collection
t	=	Time
v	=	Voltage
w	=	Velocity
w_{gas}	=	Gas average velocity
w_x	=	Transverse particle velocity
w_z	=	Horizontal particle velocity
x	=	Transverse horizontal distance
y	=	Vertical distance
z	=	Horizontal axial distance
ϵ	=	Dielectric constant
ϵ_o	=	Permittivity of free space
θ	=	Viscosity of gas
η	=	Collection efficiency
μ_i	=	Carrier mobility of the gas
π	=	3.1416
τ	=	Charging time constant
ω	=	Migration velocity parameter

The saturation charge for a nonconductive particle is

$$q_s = 12 \frac{\epsilon}{\epsilon+2} \pi \epsilon_o a_d^2 E. \tag{6}$$

The relative dielectric constant, ϵ, for a conducting particle approaches infinity and is equal to one for a perfect insulator.

The expression for the charge as a function of time is

$$q(t) = q_s \frac{t}{t+\tau}, \tag{7}$$

where τ is a charging time constant or

$$\tau = 4\epsilon_o / N_o e \mu \tag{8}$$

The particle-size range examined is larger than 0.2 μm, so the diffusion charge can be omitted.

If we start with a particle entering the field halfway between two plates and without any charge, the force balance is divided into three different components:

x - axis, the direction of the electrostatic field (transverse to gas flow)

y - axis, the direction of the gravitation force (vertically down)

z - axis, the direction of the gas flow (horizontal and axial).

The force balance is then as follows:

$$\Sigma F_x = F_{qe} - F_x - F_{ix} = 0 \tag{9}$$

$$\Sigma F_y = F_g - F_{\tau y} - F_{iy} = 0 \tag{10}$$

$$\Sigma F_z = F_{\tau z} - F_{iz} = 0 . \tag{11}$$

The electrostatic force can be expressed as

$$F_{qe} = qE . \tag{12}$$

Substituting Equations (3), (6), and (7) in Equation (12) gives

$$F_{qe} = 12 \frac{\epsilon}{\epsilon+2} \pi\epsilon \, a_d^2 \frac{t}{t + \frac{4\epsilon_o}{N_o e \mu}} \left(\frac{dv}{dr}\right)^2 0.49 , \tag{13}$$

which shows the influence of the dielectric constant, the particle size, and the field strength on the electrostatic force.

The gravitational force is

$$F_g = mg . \tag{14}$$

The viscous force, assuming Stoke's Law applies (laminar flow), is

$$F_\eta = 6\pi a_d \theta w \tag{15}$$

and the inertia force can be expressed as

$$F_i = m \, dw/dt . \tag{16}$$

If we assume that a spherical particle with a radius a is moving in this field, it will be charged to carry an amount of g (coul) charges, and the force balance in the transverse direction, after substituting Equations (12), (15), and (16) in Equation (9), becomes:

$$qE = 6\pi a_d \eta w_x - m \, dw_x/dt = 0 . \tag{17}$$

Substituting Equation (7) into Equation (17) gives

$$q_s \frac{t}{t+\tau} E - 6\pi a_d \theta w_x = m \frac{dw_x}{dt} ; \tag{18}$$

let

$$A = 6\pi a_d \theta / m \text{ and } B = q_s E/m . \tag{19}$$

Substituting this in Equation (18) and integrating gives

$$w_x = \frac{B}{A} - B\tau e^{-At} \int_o^T \frac{e^{-At}}{t+\tau} dt + C_1 e^{-At} . \tag{20}$$

The term $\int \frac{e^{-At}}{t+\tau}\,dt$ cannot be integrated but can be approximated using a series solution:

$$\int \frac{e^{-a_d x}}{b+x}\,dx = e^{-a_d b}\left[\ln (b+x) + \sum_{n=1}^{\infty} [a_d(b+x)]^n/n\cdot n!\right]$$

Then, by using this expression in Equation (20) and integrating it once more with the following initial conditions

$$t = 0,\ w_x = w_{xo} = 0 \text{ and } s_x = s_{xo} = 0\ ,$$

the travel distance s_x becomes

$$s_x = \int_o^T w_x dt = \frac{B}{A}\left(t - \frac{1}{A}(1 - e^{-At})\right) + \tau e^{-A(t+\tau)} \cdot \left[\ln \frac{t+\tau}{\tau} + \sum_{n=1}^{\infty} [(A(t+\tau)]^n - (A\tau)^n)/n\cdot n!\right] - \tau \ln \frac{t+\tau}{\tau}\ . \qquad (21)$$

The migration distance is from 0 to 15 centimeters (0 to 6 inches), and the migration time, T, needed for the particle to be collected can then be found for s_x = 15 centimeters (6 inches) by a trial-and-error solution of Equation (21).

In order to obtain the horizontal distance needed for the particles to be collected, the force balance in the z direction must be considered, i.e., Equation (10). This expression becomes

$$6\pi a_d \theta\,(w_{gas} - w_z) = m\,dw_z/dt\ , \qquad (22)$$

where $(w_{gas} - w_z)$ is the relative velocity between the particle and the gas. Integrating Equation (22), using the constants given by Equation (19) gives

$$w_z = w_{gas}\left(1 - e^{-At}\right) + w_{zo}e^{-At}\ , \qquad (23)$$

where w_{zo} is the initial particle velocity along the z-axis. The horizontal travel distance becomes, then,

$$s_z = \int_o^T w_z dt = w_{gas} \left[t + \frac{1}{A} e^{-At} - 1 \right] - \frac{1}{A} w_{zo} e^{-At} - 1 \quad . \quad (24)$$

Then, by using the travel time calculated from Equation (19), the horizontal traveling distance can be calculated as a function of particle (droplet) size and dielectric constant. With two-5 μm particles or condensed droplets, one with a dielectric constant of 2 (e.g., a condensed hydrocarbon droplet) and one with a dielectric constant of 78 (e.g., pure water droplet), migration of these two particles across a field spacing of 15 centimeters (6 inches) with an applied voltage of 50 kv and a gas velocity of 0.9 m/sec (3 ft/sec) will take a horizontal distance of 2.2 m (7.2 ft) and 1.2 m (3.9 ft), respectively. Therefore, the low dielectric particle takes almost twice the horizontal distance before being collected; this analysis points to the fact that condensable hydrocarbons (tars) and other materials with a low dielectric constant will be much more difficult to collect than conductive particles, and this has been confirmed by measurements.

When considering the removal of condensable hydrocarbons (tar mist), it should be remembered that the dielectric constants for petroleum distillates are quite low (i.e., around 2). For example, hexane (C_6H_{14}) has a dielectric constant of 2 and a boiling point of 69 C (156 F), toluene (C_7H_8) has a dielectric constant of 2.15 and a boiling point of 110 C (230 F), and naphthalene ($C_{10}H_8$) has a dielectric constant of 2.54 and a boiling point of 218 C (424 F). Other organic liquids like phenol formaldehyde resin have a dielectric constant of 6.6. Pure water has a dielectric constant of 78.

The removal efficiency of the wet electrostatic precipitator on a given gas and dust stream is a function of six basic parameters:

Collection Area
Operating Voltage
Discharge Current
Liquid-to-Gas Ratio
Treatment Time
Local Average Velocity.

The performance is often stated by the so-called migration velocity. The higher the migration velocity is, the better the particulate removal efficiency or the smaller the wet electrostatic precipitator in terms of collection area needed to treat the gas flow. The relationship between migration velocity and wet electrostatic precipitator performance is given below.

$$\omega = -V/A\ 0.508\ \ln\ (c_o/c_i)\ , \tag{25}$$

similar to the migration Equation (1).

The efficiency of the unit is given by

$$\eta = (1-c_o/c_i)\ 100\ , \tag{26}$$

and when substituting Equation (25),

$$\eta = (1-e^{(-Aw/0.508Q)})\ 100 \tag{27}$$

which is another expression for the Duetsch-Anderson Equation (2).

The migration velocity ω is a performance parameter that does not in reality relate directly to the speed at which the particles migrate to the collecting plates. It is a "catch-all" which also includes all operating parameters not included in Equation (25).

HORIZONTAL-FLOW WET ELECTROSTATIC PRECIPITATOR

One of the wet electrostatic precipitators can be characterized as a continuously sprayed, horizontal-flow, parallel-plate, and solid-discharge electrode type. In terms of gaseous absorption, it can be characterized as a combination cocurrent and a cross-flow scrubber.

In the application of a wet electrostatic precipitator, it is very important that the gas to be treated is saturated with water vapor to prevent the water inside the wet electrostatic precipitator from evaporating, which causes loss of washing water and dry zones on the internal members. The saturation of the gas can be done in a spray tower or scrubber upstream of the wet electrostatic precipitator, or it can be done in the inlet section of the wet electrostatic precipitator, or both.

In addition, it is also necessary to obtain a uniform velocity profile across the wet electrostatic precipitator, and the diffusion of the flow from the inlet duct velocity down to the wet electrostatic precipitator face velocity has to be performed in the inlet section. Furthermore, by spraying cocurrent into the inlet section, some of the coarser particles will be removed and the gas-absorption process will be started. To accomplish this, sections of baffles and sprays are located in the inlet cone of the wet electrostatic precipitator.

After passing through the sections of transverse baffles, the dirty gas stream then enters into the first electrostatic field. Water sprays located above the electrostatic-field sections introduce the proper amount of water droplets to the gas stream for washing of internal surfaces. The particulates and the water droplets in the electrostatic field pick up a charge and migrate to the collecting plates. The collected water droplets form a continuous downward-flowing film over all the collecting plates and keep them clean. The water film and the collected particulates flow down the collecting plates into the troughs below, which are sloped to a drain.

The transverse-baffle gas-distribution system combined with the extended electrode, located upstream and downstream of each field, insures complete gas-flow uniformity from passage to passage, and collects particulates and droplets by impingement, and by electrostatic forces. Also, the extended discharge electrode system improves the collection efficiency by increasing effective collection area. At the entry of a field, particles not captured by the transverse baffles are given an advance charge by the forward extended electrode before they come into proximity of the collecting plates. Thus charged, the particles start immediately to migrate toward the leading edge of the plates. It has been found that the downstream side of the baffles at the exit of a field collects a considerable amount of material. The very small charged particles escaping the parallel-plate field are pulled into the wake of the baffles by the slight vacuum resulting from the turbulent dissipation of energy. Since the particles have an electrostatic charge, some of them will be collected on the back side of the baffles.

All baffles systems are arranged so that a walkway runs across the front and the back of each of the electrostatic fields. The discharge electrode frames are mounted on collar-type, high-voltage support insulators. Insulator compartments are heated and pressurized to prevent moisture and particulate leakage into the insulator compartment.

In any particulate and/or gaseous removal process where a liquid is used, it is important to remove the carryover liquid drops and mists before reaching the outlet of the equipment. It has been found that doing this electrostatically is highly efficient. Hence, the last section is operated dry, thereby establishing an electrostatic barrier that the liquid droplets cannot penetrate. The mist collects on the front side of the baffles, and the downstream side is dry. However, some small dust particles can penetrate and these will collect on the downstream baffles. Therefore, this surface is washed intermittently to prevent buildup of particulates.

RANGE OF APPLICATIONS

During the past 2 years, many new applications have been piloted and units have been sold and installed following successful pilot-plant work. The wet electrostatic precipitator can be used for applications on gas streams containing relatively light dust loading of submicron particles and/or condensed organic materials forming a submicron fume. Ordinarily these applications would require very-high-pressure-drop scrubbers. The energy consumption and operating costs are less than what would be needed to operate scrubbers. The water-treatment requirements for the wet electrostatic precipitator would be the same as those for scrubbers.

In some applications, where the dust resistivity is either very high or very low, the wet electrostatic precipitator can also be applied successfully in competition with dry electrostatic precipitators.

Wet electrostatic precipitators have been installed for the following applications:

(1) On Soderberg aluminum reduction cells (pot lines), both of the vertical and horizontal stud type, for simultaneous removal of aluminum oxides, solid and gaseous fluorides, tar mist (condensable hydrocarbons), and SO_2

(2) On carbon-anode baking furnaces for removal of carbon particles, tar mists, and SO_2

(3) On fiber-glass resin application section and forming lines for removal of short broken glass fibers, phenolic resins, and tars

(4) In molybdenum sulfate roasting, downstream of a scrubber for removing ammonium sulfite – sulfate aerosols which form in the ammonia scrubbing process and SO_2.

Wet electrostatic precipitators are now being manufactured and installed

(1) For upgrading of low-pressure-drop scrubbers on phosphate rock driers for removal of the submicron particles and SO_2

(2) On coke-oven batteries when connected to a continuous shed or hood along the push side of the battery where the coke is pushed into the railroad car. Here the wet electrostatic precipitator will remove the fine carbon particles and the condensable hydrocarbons during the push cycle. In addition, the wet electrostatic precipitator will collect any emissions caused by door leakage on the push side.

A wet electrostatic precipitator has been designed to meet the requirements for controlling reclamation (sinter) plant emissions.

Reclamation (Sinter) Plant Design Specifications

Table 10 provides information concerning a wet electrostatic precipitator for controlling emissions from a sinter plant producing about 2,300,000 metric tons (2,530,000 net tons) of high-basicity sinter annually. *

Reclamation (Sinter) Plant Electrostatic Precipitator Design Data

There is very little specific design information available in the published literature relating to the design of reclamation (sinter) plant electrostatic precipitators. Information presented in this section is indicative of the data that have been published.

Particulate Characteristics–The electrical resistivity of the particulates is an important design factor, and an example of the variations in electrical resistivity as affected by the temperature of the gas and the sinter mixture is shown in Figure 22. (55)

*Used with the permission of MikroPul Corporation, November 27, 1974.

TABLE 10. EQUIPMENT SPECIFICATIONS

Gas Conditioner (Absorber) Specifications

Operating Data		
Inlet Volume	8,496 actual cu m/min	300,000 actual cu ft/min
Inlet Temperature	202-204 C	395-400 F
Inlet Moisture Content:		
Percent Volume	12	12
Humidity	0.3839 kg water vapor/kg dry gas	0.8464 lb water vapor/lb dry gas
Inlet Gas Density	0.7106 kg/cu m	0.04436 lb/cu ft
Outlet Volume (Saturated)	6,519 actual cu m/min	230,000 actual cu ft/min
Outlet Temperature	60 C	140 F
Outlet Humidity	0.069 kg water vapor/kg dry gas	0.153 lb water vapor/lb dry gas
Outlet Gas Density	0.9817 kg/cu m	0.06128 lb/cu ft
Inlet Particulate Loading	0.1961 gram/cu m	0.0857 grain/dry std cu ft
Inlet Condensable Loading	0.2591 gram/dry cu m	0.1132 grain/dry std cu ft
Total Inlet Loading	0.4552 gram/dry cu m	0.1989 grain/dry std cu ft
Expected Outlet Particulate Loading	0.0785 gram/dry cu m	0.0343 grain/dry std cu ft
Expected Outlet Condensable Loading	0.1943 gram/dry cu m	0.0849 grain/dry std cu ft
Total Expected Outlet Loading	0.2728 gram/dry cu m	0.1192 grain/dry std cu ft
Pressure Drop Across Absorber	2.54 cm water gage	1.0-inch water gage
Gas Velocity	2.92 m/sec	9.59 ft/sec
Treatment Time	+1.88 sec	+1.88 sec
Number of Absorbers	Two (2)	Two (2)

Precipitator

Operating and Performance Data		
Volume at saturated conditions	3,260 cu m/min	115,100 cu ft/min
Temperature at saturated conditions	60 C	140 F
Inlet Loading		
Particulate	0.0785 gram/dry cu m	0.0343 grain/dry std cu ft
Condensable	0.1943 gram/dry cu m	0.0849 grain/dry std cu ft
Total	0.2728 gram/dry cu m	0.1192 grain/dry std cu ft
Guaranteed Overall (Absorber and Precipitator) Efficiency, percent	92.45	92.45
Guaranteed Total Outlet Loading	0.03 gram/dry cu m	0.015 grain/dry std cu ft
Pressure Drop Across Precipitator Including Gas Distribution Devices, but excluding losses across dampers	127-mm water gage	5.0-inch water gage
Gas Velocity	0.472 m/sec	2.73 ft/sec
Treatment Time	8.79 sec	8.79 sec

TABLE 10. (Continued)

Precipitator		
Arrangement		
Number of Precipitators	4	4
Chambers (Number)/Precipitator	1	1
Fields (Number and Length)/ Precipitator	3, 183 m	3, 6 ft
Casing Material and Thickness	6.35 mm	1/4-inch mild steel
Casing Design Pressure - Positive	254-mm water gage	10-inch water gage
Number of Hoppers per Precipitator	3	3
Hopper Material and Thickness	6.35 mm	1/4-inch mild steel
Type of Hopper	Sloping	Sloping
Insulator Compartment Materials and Thickness	2.72 mm	12-gage mild steel
Number of Insulator Compartments per Precipitator	6	6
Precipitator Internal Gas Distribution Devices		
(a) Types	Transverse baffles	
(b) Quantity and Location per Precipitator	Two sets - inlet nozzle One set - inlet 1st field Two sets - between stages One set - mist eliminator	
(c) Material and Thickness	1.56 mm, X18H11M	16-gage, Type 316
Number, Type, and Size of Access Doors per Precipitator		
(a) Roof	5, 0.61 m x 1.37 m	2 ft x 4.5 ft
(b) Shell	2, 0.61 m x 1.37 m	2 ft x 4.5 ft
(c) Insulator Compartments	6, 0.61 m x 1.37 m	2 ft x 4.5 ft
(d) Inlet	1, 0.61 m x 1.37 m	2 ft x 4.5 ft
(e) Outlet	1, 0.61 m x 1.37 m	2 ft x 4.5 ft
Access Walkways Internal	Mild steel expanded metal grating between fields	
Collecting System - per Precipitator		
Number of Gas Passages	29	
Spacing of Gas Passages	30.5 cm	12 inches
Collecting Plate Material and Thickness	1.95 mm, X18H11M	14-gage, Type 316
Collecting Plate Effective Length	5.5 m	18 feet
Collecting Plate Effective Height	7.6 m	25 feet
Active Collecting Surface Area	2,341 sq m	25,200 sq ft
Plate Area		
Transverse Baffle Section Area	390 sq m	4,200 sq ft
Total	2,731 sq m	29,400 sq ft

TABLE 10. (Continued)

	High Voltage System	
Discharge Electrode - Type, Material and Thickness	3.11 mm, 1X16M13ME	11-gage, Type 316L
	High Voltage Electrical Set	
Type Transformer Rectifier	Silicon	
Number of Transformer Rectifiers	3/unit	
(a) Voltage Rating, kv (dc) avg.	55	
(b) Current Rating, ma (dc) avg. (for pure resistive loads)	1,000	
Number of Transformer Rectifier Control Cabinets	1/unit	
Construction of Transformer Rectifier Control Cabinets	NEMA 12	
Transformer Rectifier Insulation Fluid	Pyranol	
Wave Form of High Voltage	Full Wave	
Number and Type of High Voltage Switches	3/Grounded	
Key Interlocks		
Control Cabinets	Yes	
Transformer Rectifiers	Yes	
Access Doors	Yes	
Type of Transformer Rectifier Controls	Thyristor	
Maximum Ambient Temperature for Transformer Rectifier, C	40	
Connected Load kva/Precipitator		
Transformer-Rectifier	235	
Insulator Heater and Blower	28	
Total Connected Load KVA/ Precipitator	263	
Power Distribution		
Individual Breakers Each Control Cabinet	Yes	
Central Distribution Panel	No	

Operating Liquid Characteristics for Precipitator and Absorber

	Absorber Feed		Precipitator Feed	
Liquor Rate	5678 l/min	1500 gal/min	2839 l/min	750 gal/min
Liquor Pressure at Nozzles	293 kg/sq m	60 lb/sq in. gage	293 kg/sq m	60 lb/sq in. gage
Liquor Source	pH-Controlled Recycled Treated Liquor			
Evaporation Rate	378 l/min	100 gal/min	--	--

TABLE 10. (Continued)

Operating Liquid Characteristics for Precipitator and Absorber

	Absorber Feed	Precipitator Feed
Liquor Quality: The following typical liquor quality observed during the pilot-plant study is required for efficient absorber and precipitator operation.		
pH	9.6	9.2
	mg/l	mg/l
Phenophthalein Alkalinity as $CaCO_3$	1,450	1,390
Methyl Orange Alkalinity as $CaCO_3$	3,800	3,410
Chloride as Cl	240	194
Sulfate as SO_4	3,750	3,650
Hardness as $CaCO_3$	24	25
Calcium as $CaCO_3$	3	8
Magnesium as $CaCO_3$	16	17
Silica as SiO_2	10.5	10.1
Total Solids	10,652	10,224
Dissolved Solids	10,488	10,090
Suspended Solids	164	134
Total Iron as Fe	7.9	6.4
Aluminum as Al	1.8	1.6
Zinc as Zn	0.4	0.3
Lead as Pb	6.5	3.9
Cadmium as Cd	0.18	0.10
Molybdenum as Mo	1	1
Fluoride as F	42	40
Oil and Grease	79	108
Total Carbon	570	300
Total Inorganic Carbon	420	200
Total Organic Carbon	150	100

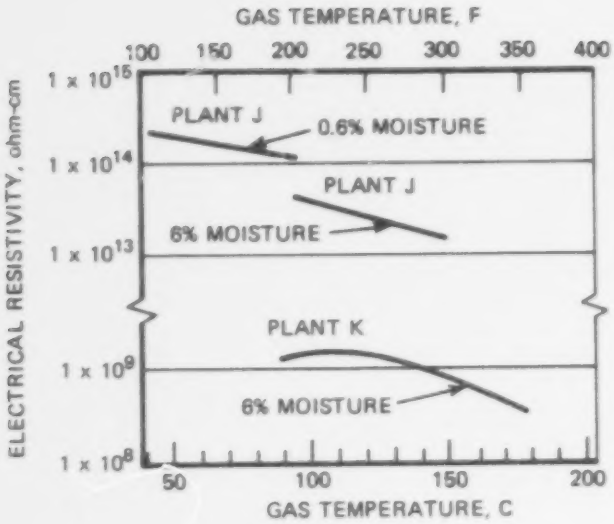

Figure 22. Electrical resistivity of reclamation (sinter) plant dust as affected by gas temperature and sinter mixture

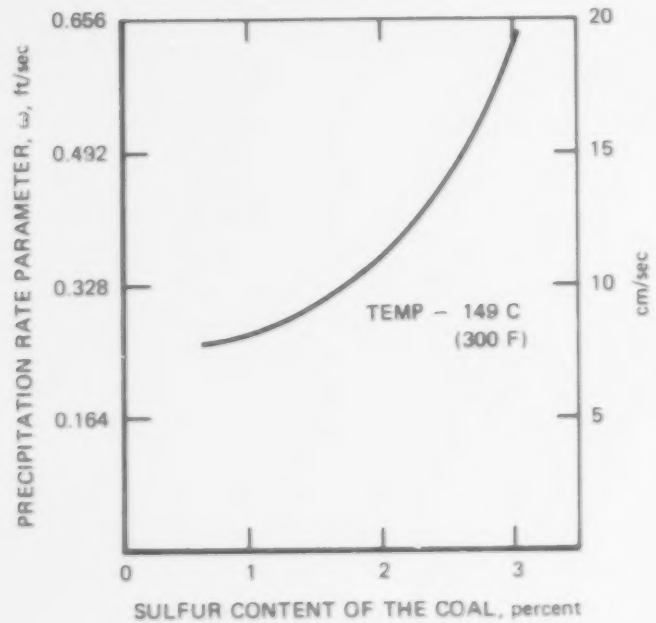

Figure 23. Relationship between the sulfur content in electric-utility-plant coal and the precipitation-rate parameter

Sinter mix composition, particulate size, and gas data are listed in Table 11.[56]

TABLE 11. RECLAMATION (SINTER) PLANT DATA FOR FIGURE 22

Parameter	Plant J	Plant K
Sinter Mixture		
Iron ore and metallics, percent	90	64
Limestone or dolomite, percent	9	35
Coke, percent	1	1
Particle Size, percent -10 microns	60	45
Gas Analysis		
Sulfur oxides, ppm	300	30
Moisture content, percent	15	10
Temperature	121 C (250 F)	93 C (200 F)

It is known that the sulfur content of reclamation-plant off-gas affects the collection of emissions. While such data are not available for reclamation-plant off-gas, Figure 23 shows the relationship between the sulfur content in fuel and the precipitation-rate parameter ω for electric-utility electrostatic precipitators.[55]

The effect of various reclamation (sinter)-plant electrostatic-precipitator variables on collection efficiency is shown in Figure 24.[57]

The limited amount of information available on reclamation (sinter)-plant electrostatic precipitators is given in Table 12.[34,54,55,58,59]

Reclamation (sinter) plant electrostatic precipitators are typically single-stage, horizontal-flow units. The chambers and hoppers are usually fabricated of plain-carbon steel, and may or may not be thermally insulated.[55] Plain-carbon steels have not performed as well as desired because of the corrosive conditions that can be generated by the reaction of sulfur oxides with moisture to form acids. This acid corrosion necessitates the replacement of electrodes, collector plates, and internal supporting members, causing excessive maintenance costs and short service life, as compared with other equipment used in an iron and steel plant.

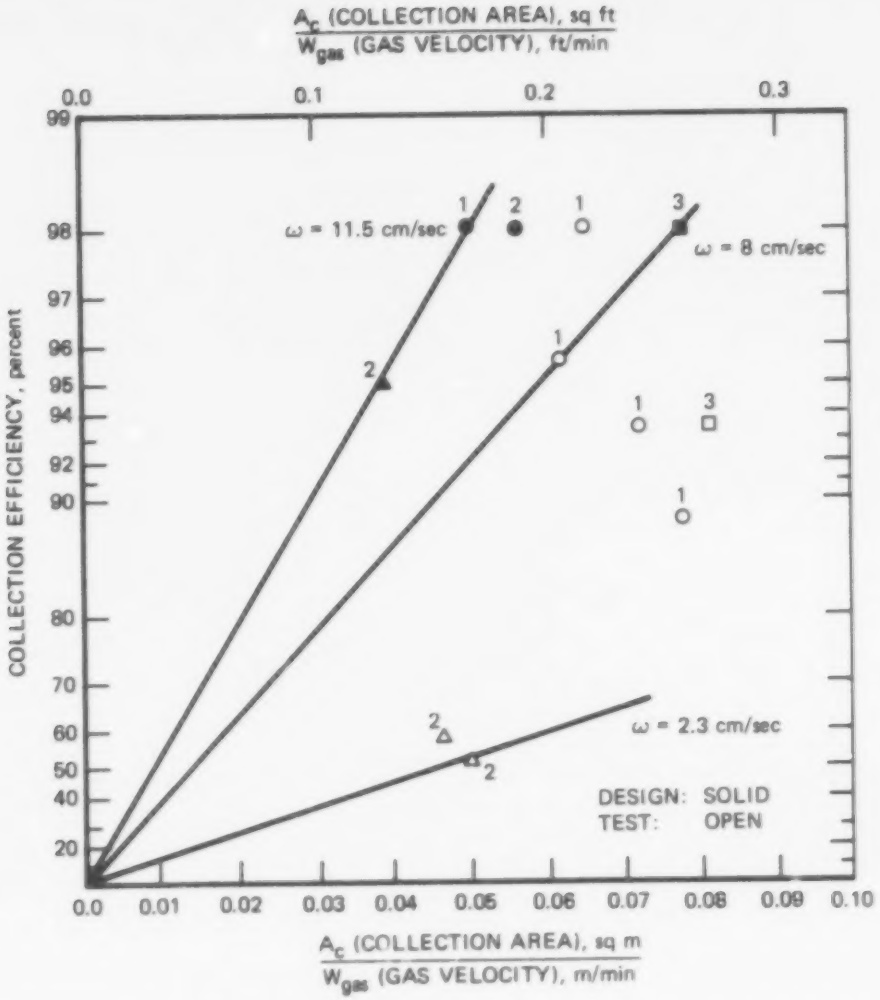

Figure 24. Collection efficiency as affected by the ratio of collection area to gas velocity

TABLE 12. RECLAMATION (SINTER) PLANT ELECTROSTATIC-PRECIPITATOR CHARACTERISTICS

Plant Location	Bethlehem Steel Corp., Johnstown, Pennsylvania	Inland Steel Co., East Chicago, Indiana	Plant L, Eastern Pennsylvania	Plant I Reference (54)
Annual Production				
metric tons	998,000	1,089,000	454,000	2,177,000
net tons	1,100,000	1,200,000	500,000	2,400,000
Strands, number	2	1	1	4 (2 per ESP)
Air Volume				
cu m/sec	100	215	80	180
cu ft/min	213,000	457,000	170,000	385,000
Air Temperature				
C	115	191	149	118
F	240	375	300	245
Pressure Differential				
kg/sq m	762	889	660	1070
inches of water	30	35	26	42
Gas Velocity				
cm/sec		195		174
ft/sec		6.4		5.7
Treatment Time, seconds		2.3		4.2
Charge Section				
Number of Ducts	37			
Width				
centimeters	23			
inches	9			
Height				
meters	7.3			
feet	24			
Length				
meters	2.7			
feet	9			
Number of Electrodes	456			
Size				
mm^2	6			
$in.^2$	0.0093			
Type of Suspension	Plumb Bob			
Power				
Collection Section				
Number of Plates	76	136	70	
Height				
meters		2.3	1.8	
feet		7.5	6.0	
Length				
meters		7.3	7.3	
feet		24.0	24.0	
Number of Electrodes	872			1600

VI. REFERENCES

(1) Annual Statistical Report, American Iron and Steel Institute, 1974, pp. 65, 72.

(2) Ess, T. J., Alan Wood Steel Company, Iron and Steel Engineer, 39: AW4-AW22, March 1962.

(3) Annual Report, Alan Wood Steel Company, 1972.

(4) Fosdick, A. H., Operating Features and Practices at the Bethlehem Sintering Plant. AIME Blast Furnace, Coke Oven, and Raw Materials Proceedings. 7:106-118, 1948.

(5) Gas Cleaning System for Bethlehem's Sintering Plant. Blast Furnace and Steel Plant. 59:60, January 1971.

(6) The Bethlehem Plant's New $2.4-Million Stack Gas Cleaning System. American Metal Market, p. 6, December 9, 1970.

(7) Sinter Line Baghouse Collector Still Going Strong. Iron and Steel Engineer. 45:124, February 1968.

(8) Ess, T. J. Bethlehem's Johnstown Plant. . . A Century of Pioneering. Iron and Steel Engineer. 30:J2-J20, April 1953.

(9) Air Pollution Control System Installed at Bethelehem's Johnstown Plant. Blast Furnace and Steel Plant. 56:917, October 1963.

(10) Lassen, E., Jones and Laughlin Steel Corporation's Aliquippa Works. Blast Furnace and Steel Plant. 54:957-958, October 1966.

(11) J & L Operating Largest Single Strand Iron Ore Sintering Line. Industrial Heating. 28:1682-1690, September 1961.

(12) Air Pollution Control Continues at J&L Aliquippa Works. Industrial Heating. 31:486,500, March 1964.

(13) Communication from R. C. McCrillis, Environmental Protection Agency. April 25, 1975.

(14) Harris, E. R., and Beiser, F. R. Cleaning Sinter Plant Gas With a Venturi Scrubber. Journal of the Air Pollution Control Association. 15:46-49, February 1965.

(15) Communication from B. Steiner, April 9, 1975.

(16) Air Emission Control Facility at United States Steel Corp.'s Saxonburg, Pa., Sintering Plant. Iron and Steel Engineer. 46:45, April 1969.

(17) Faigen, M. R., Kyler, E. B., and Plummer, W. S. Recent Improvements at United States Steel – Saxonburg Sinter Plant. AIME Ironmaking Proceedings. 29:310-318, 1970.

(18) To Add Sinter Plant at Monessen Works. Iron and Steel Engineer. 41: 50, April 1964.

(19) Edwards. L. H. Equipment and Operational Changes Made to Upgrade an Old Sinter Plant. AIME Ironmaking Proceedings. 29:328-333, 1970.

(20) Two J&L Sintering Machines Served by Vertical Shaft Sinter Cooler. Industrial Heating. 28:514-516, March 1961.

(21) Kraner, H. M., and Hauser, R. E. New Sintering Plant Facilities at Sparrows Point. Blast Furnace and Steel Plant. 44:757-759, July 1956.

(22) Largest in Western Hemisphere. Journal of Metals. 24:8, June 1972.

(23) Watson, G. W. Weirton No. 2 Sinter Plant. Iron and Steel Engineer. 36:105-108, June 1959.

(24) Cleaning System Turnkey Contract. American Metal Market. p. 14, September 3, 1971.

(25) Communication from B. Steiner. June 25, 1975.

(26) Loofboro, K. A. J&L's Cleveland Works Sinter Plant. Iron and Steel Engineer. 36:101-104, June 1959.

(27) Ess, T. J. Republic Builds for D.P.C. Iron and Steel Engineer. 21:R18-R38, October 1944.

(28) Republic Steel Plants and Facilities. Republic Steel Corporation. 28 p. February 1967.

(29) Austermiller, E. O., and Cureton, W. A. Design and Operation of National Tube's Sintering Plant. Iron and Steel Engineer. 28:111-117, October 1951.

(30) Slater, R. A. Construction and Design Involved in a New Sintering Plant. Iron and Steel Engineer. 37:114-117, December 1960.

(31) Cromwell, D. P. Operations and Practice, Campbell Sintering Plant. AIME Blast Furnace, Coke Oven, and Raw Materials Proceedings. 7:86-89, 1948.

(32) Armco Completes Sintering Unit at Ashland Plant. Iron and Steel Engineer. 35:146-152, October 1958.

(33) Baranyi, J. F. Results of Design Changes in Sinter Plants. Iron and Steel Engineer. 42:85-90, December 1965.

(34) Frame, C. P., and Elson, R. J. The Effects of Mechanical Equipment on Controlling Air Pollution at No. 3 Sintering Plant, Indiana Harbor Works, Inland Steel Company. Journal of the Air Pollution Control Association. 13:600-603, December 1963.

(35) Inland Steel Shuts Down Two Sintering Lines at Indiana Harbor Works. Blast Furnace and Steel Plant. 55:660, July 1967.

(36) Young, T. A., Jr. Gary Steel Works Experience With Dust Control at Number 3 Sinter Plant. Blast Furnace and Steel Plant. 56:1057-1063, December 1968.

(37) Bethlehem Tells Details of Proposed Sintering Plant. American Metal Market. p. 4, November 2, 1972.

(38) Bayr, R. B., and Wachowiak, R. J. Elimination of Hydrocarbon Emissions From the Sinter Plant. AIME Ironmaking Proceedings. 31:55-58, 1972.

(39) A New $700,000 Baghouse. Skillings Mining Review. 64(18):28, May 3, 1975.

(40) Corzilius, W. R. Sintering Plant Expands Blast Furnace and Open Hearth Capacity. Blast Furnace and Steel Plant. 47:44-50, January 1959.

(41) Sinter Plant Baghouse Cleaner for Granite City Steel. Blast Furnace and Steel Plant. 59:241, April 1971.

(42) Scrubber System For Granite City. American Metal Market. p. 6, December 4, 1973.

(43) Pollution Control Project. American Metal Market. p. 4, September 4, 1970.

(44) A New Baghouse Type Dust Collecting System. American Metal Market. p. 3, December 28, 1970.

(45) Menke, G. V. Sintering Plant Emission Control Wisconsin Steel Works. Preprint AIME Ironmaking Conference. 10 p. 1972.

(46) CF&I Steel Installing Electrical Precipiators To Control Iron Ore Dust At Its Pueblo Plant. Blast Furnace and Steel Plant. 57:82, January 1969.

(47) Egley, B. D. Selection of Gas Cleaning Equipment For an Ore Preparation Plant. Iron and Steel Engineer. 47:111-115, November 1970.

(48) Kaiser Steel Starts Operation of New Pollution Control Unit. American Metal Market. p. 18, August 9, 1971.

(49) Nowak, T. T. Sinter Plant Baghouse. AIME Ironmaking Proceedings. 31:75-84, 1972.

(50) Communication From R. L. Bump, Research-Cottrell, Inc., to J. Varga, Jr. July 31, 1975.

(51) McCrone, W. C., et. al. The Particle Atlas. Ann Arbor Science Publishers, Inc. Ann Arbor, Michigan. 153-236, (1967).

(52) Manning, G. E., and Rower, F. E. A Characterization of Air Pollutants From Sintering Plant Induced Draft Stacks. AIME Ironmaking Proceedings. 30:452-460 (1971).

(53) Suitlas, J. R. Emission Characteristics and Pilot Plant Studies on a Sintering Plant Windbox Discharge. AIME Ironmaking Proceedings, 30:461-470 (1971).

(54) Communication from R. C. McCrillis to J. Varga, Jr.

(55) Oglesby, S., Jr., and Nichols, G. B. A Manual of Electrostatic Precipitator Technology, Part II – Application Areas. The National Air Pollution Control Administration, Division of Process Control Engineering. PB 196381. 487-502 (August 25, 1970).

(56) Bakke, E., The Application of Wet Electrostatic Precipitators for Control of Fine Particulate Matter, Paper presented at the Symposium on Control of Fine Particulate Emissions From Industrial Sources for the Joint U.S.-U.S.S.R. Working Group, Stationary Source Air Pollution Control Technology. San Francisco, California. 27 pp. (January 15-18, 1974).

(57) Oglesby, S., Jr., and Nichols, G. B. A Manual of Electrostatic Precipitator Technology, Part I – Fundamentals. The National Air Pollution Control Administration, Division of Process Control Engineering. PB 196380. 203-217 (August 25, 1970).

(58) Communication from R. C. McCrillis to J. Varga, Jr. April 25, 1975.

(59) Communication from W. McShane to J. Varga, Jr. July 11, 1975.